

Introduction 6

**INTRODUCTION TO
THE DEEP OCEAN** 10

OCEANOGRAPHY 42

DEEP-SEA ORGANISMS 76

HABITATS 122

GLOBAL PATTERNS 178

**HUMANITY AND
THE DEEP OCEAN** 230

Classification of deep-sea species 278

Glossary 280

Resources 282

Notes on contributors 283

Index 284

Acknowledgments 288

Surveying and exploring the seafloor

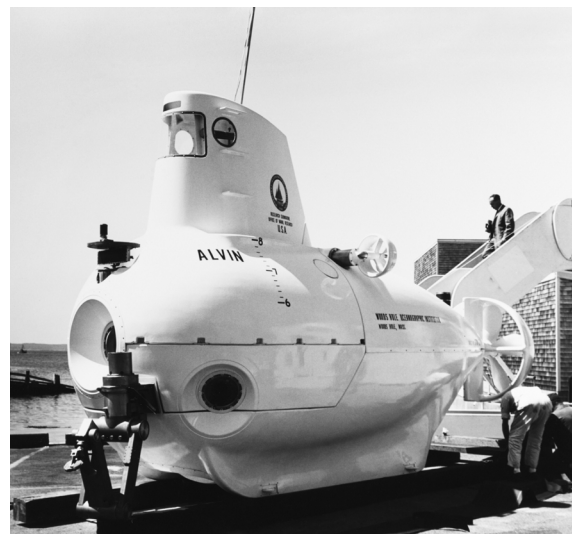
Mapping of the physical geography of the ocean floors made great strides in the mid-20th century. In 1957, geologist Bruce Heezen and cartographer Marie Tharp began producing physiographic maps of all the oceans, showing the extensive mid-ocean ridge system. In 1963, paleogeomagnetic studies by geophysicists Lawrence Morley, Frederick Vine, and Drummond Matthews provided the first direct evidence of seafloor spreading from the mid-ocean ridges. By the end of the decade, the theories of continental drift and plate tectonics were generally accepted. In 1997, geophysicists Walter Smith and David Sandwell produced new global high-resolution maps of the ocean floor using satellite data.

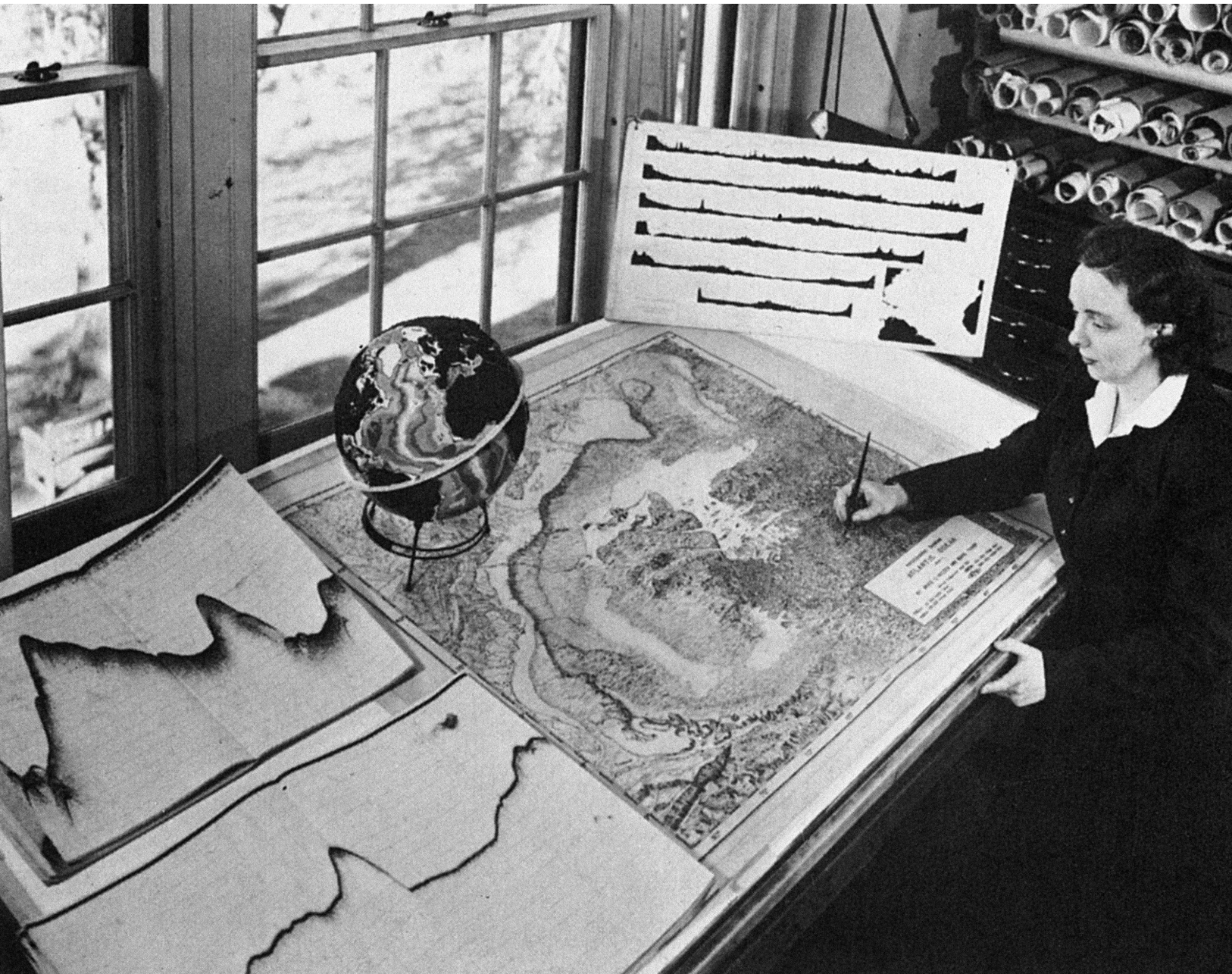
The mid-20th century also saw development of two types of submersibles, human-occupied vehicles (HOVs) and remotely operated vehicles (ROVs). These vessels increasingly provided scientists with direct access to the deep sea and the seafloor, opening up the possibilities for discovery. In 1960, explorers Jacques Piccard and Don Walsh reached the deepest point in the world ocean, the Challenger Deep, in the bathyscaphe *Trieste*.

The Woods Hole Oceanographic Institution (WHOI) improved on the bathyscaphe model with *Alvin*, launched in 1964, a more maneuverable submersible that contained imaging and sampling gear that enabled scientists to make new discoveries in the deep sea. In 1966, *Alvin* allowed WHOI biologist Richard Backus and others to directly observe that deep scattering layers in the Pacific Ocean were made up of vast numbers of mesopelagic fishes (see Pelagic Fishes, pages 104–109). With the assistance of *Alvin*, a team of researchers including oceanographers Jack Corliss and Bob Ballard discovered chemosynthetic life at hydrothermal vents in the Pacific Ocean in 1977. Similar chemosynthetic organisms were discovered via submersibles at hydrocarbon cold seeps by marine geologist Charles Paull and others in 1984. With both these discoveries, scientists realized that the deep sea contains a variety of specialized communities thriving in the absence of energy input from the sun (see Chemosynthetic Ecosystems, pages 158–167).

Discoveries made on the sea surface also informed studies of the deep. In 1980, the space engineer Warren Hovis and others published the first satellite images of sea-surface chlorophyll, and it became possible to produce global maps of sea-surface primary production and to quantify the flux of organic matter to the deep sea. Geoscientist Susumu Honjo of WHOI, in 1976, pioneered complementary direct measurement of flux by time-series sediment traps moored at different depths below the surface. These initiatives resulted in global programs of remote sensing and flux studies of the deep sea.

Today, exploration and discovery continue, including recognition of new deep-sea species by numerous individuals and institutions. Recent international coordination efforts have included the Census of Marine Life (CoML, 2000–2010), which studied marine biodiversity and abundance in the world's seas and oceans.





Bathyscaphe Trieste

Preparations prior to the first dive to the deepest point in the world's oceans on January 23, 1960. Jacques Piccard, the designer, and US Navy officer Don Walsh spent 20 minutes at the bottom of the Mariana Trench.

DSV Alvin

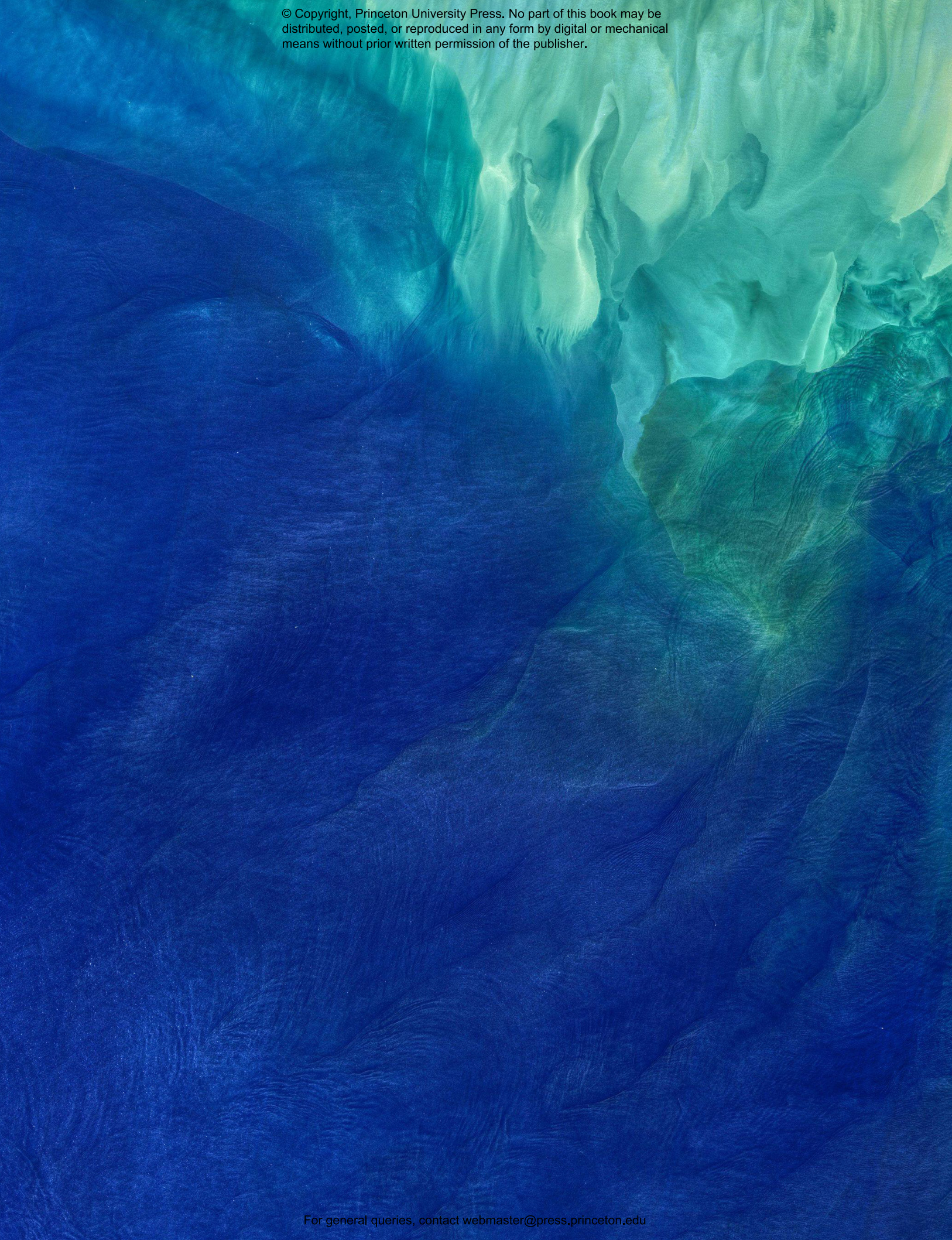
The first of a new class of human-occupied deep submergence vehicles delivered on June 5, 1964. It was capable of powered maneuvering in three dimensions down to 7,870 ft. (2,400 m). Recent versions of *Alvin* and other HOVs can reach much greater depths.

Mapping the ocean floor

Marie Tharp, geologist and oceanographer, constructing a map of the Atlantic Ocean floor in the 1950s. Discovery of the global mid-ocean ridge system contributed to the theories of continental and plate tectonics.

“Human-occupied vehicles (HOVs) and remotely operated vehicles (ROVs) provided scientists with direct access to the deep sea and the seafloor, opening up the possibilities for discovery.”

© Copyright, Princeton University Press. No part of this book may be distributed, posted, or reproduced in any form by digital or mechanical means without prior written permission of the publisher.



© Copyright, Princeton University Press. No part of this book may be distributed, posted, or reproduced in any form by digital or mechanical means without prior written permission of the publisher.

An aerial photograph of a coastal region. On the right side, a dense, green forested landmass is visible. A large, light-colored river delta with multiple channels flows from the land into a bay. The water in the bay is a pale turquoise color, while the open ocean to the left is a deep, dark blue. A small island or peninsula is visible in the lower part of the bay. A large black circle is superimposed over the center of the image, containing the word 'OCEANOGRAPHY' in white capital letters.

OCEANOGRAPHY

For general queries, contact webmaster@press.princeton.edu

UNDERWATER TOPOGRAPHY

Continents, plates, ridges, and subduction zones

About 3.8 billion years ago, the ocean most likely formed from the escape of water vapor and other gases from molten rocks to the atmosphere surrounding the cooling planet. Debate is ongoing whether comets, specifically those of a type known as “hyperactive,” contributed some of the earth’s water. Once the earth cooled below 212°F (100°C), water vapor condensed into rain, which filled the basins that we know now as our world ocean. Gravity prevented the water from leaving the planet.

Continental and oceanic plates

The earth’s surface is divided into eight major and several minor tectonic plates—large, rigid pieces of the planet’s crust and upper mantle. These plates are of two primary types: continental plates and oceanic plates. Of the major plates, the largest, the Pacific Plate, is the only one that is nearly entirely oceanic; it supports some tropical islands as landmasses above water. However, as landmasses take up only 30% of the earth’s surface, most of the continental plates are about half above water and half under, forming substantial expanses of deep seafloor. For example, both the North American and South American tectonic plates reach well eastward under the ocean to the Mid-Atlantic Ridge, forming the Atlantic Ocean floor. The Australian Plate contains portions of both the Indian Ocean floor and the Pacific Ocean floor.

While the two types of plates share many characteristics, several differences distinguish them. Oceanic plates average about 4–5 mi. (6–8 km) thick, compared to an average of 25 mi. (40 km) for continental plates. Oceanic plates are composed of basalt rich in iron, magnesium, and calcium. Continental plates are dominated by granitic rock with abundant silica, aluminum, sodium, and potassium. Because of their heavy ferromagnesian elements, oceanic plates are about one-fifth denser than continental plates. This difference in density causes oceanic plates to descend (or subduct) beneath the lighter continental plates when they meet. It also allows the denser oceanic plates to sink farther into the earth’s upper mantle, causing them to lie below sea level. The more buoyant continental plates float higher on top of the mantle, resulting in dry land.

Previous pages: **Internal waves**

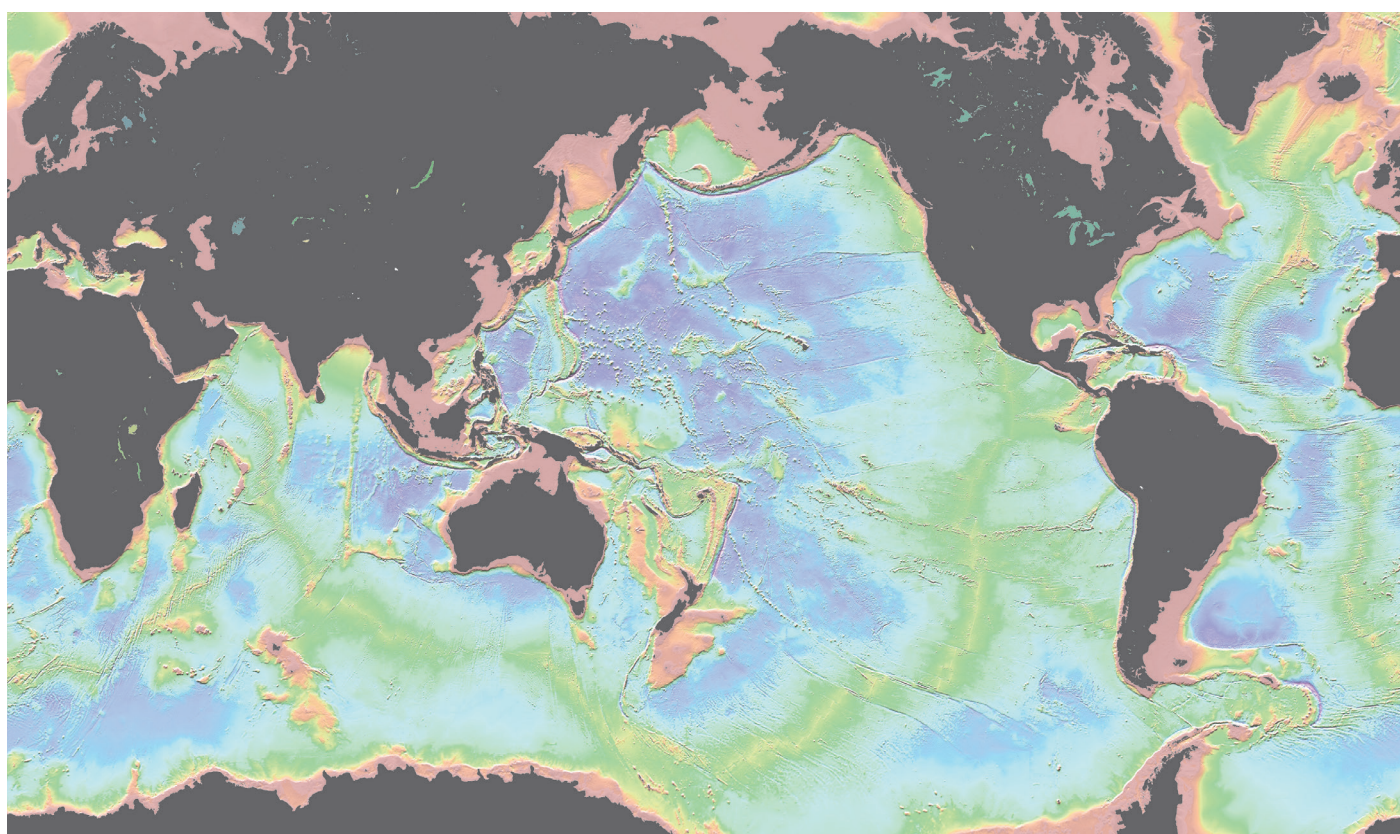
Satellite image of the Andaman Sea, off the coast of Thailand. Internal waves can be hundreds of meters tall and tens to hundreds of kilometers long—and yet moving all the way to the deep sea beneath the sea surface. The sunlight helps make the internal waves visible (patterns and ripples in the center of the image)—the waves in the deep displace the surface by about 4 in. (0.1 m).

Major tectonic plates

The division of tectonic plates on the earth’s surface. The Pacific Plate is the largest.

Seafloor spreading ridges

The topography of the earth reveals the seafloor spreading ridge system at a depth of 8,200 ft./ 2,500 m (yellow). Deep ocean trenches (purple) are the sites where the cool and dense plates sink into the earth. The abyssal plains are shown in dark blue.



Ridges and subduction zones

Oceanic plates are formed at divergent plate boundaries along mid-ocean ridges, where upwelling magma creates new oceanic crust. As lava flows from these volcanic ridges, it quickly cools, forming igneous rock. The spread of the Atlantic Ocean at the Mid-Atlantic Ridge, a large chain of volcanic seamounts, all lying underwater except for a few islands, is about 1 in. (2.5 cm) per year. Continental plates are formed primarily by converging plate boundaries, where oceanic plates collide with, and plunge underneath, continental plates—a process called subduction. As oceanic plates subduct, they melt to form magma. This magma cools over millions of years, producing new continental crust.

Oceanic and continental plates differ considerably in age because of plate tectonics, processes that control the structure and properties of the earth's crust and its evolution through time. Divergent plate boundaries continually renew oceanic plates, while the subduction zones of convergent boundaries continually recycle them. As a result, the oldest oceanic rocks are less than 200 million years old. In contrast, continental plates take a long time to form but are rarely destroyed. Much of the continental crust exceeds 1 billion years in age, and its oldest rocks may be as old as 4 billion years.

The subduction zones lead to the deepest points on Earth: the hadal trenches, which exceed 19,700 ft. (6,000 m) in depth. Trenches deeper than 27,500 ft. (8,400 m) are found only in the Pacific Ocean. Along the perimeter of the Pacific oceanic plate are numerous deep spots; the deepest, down to around 32,800 ft. (10,000 m), are found only on its western side. Ocean trenches also show variation in topography and thus in depth. For example, the Mariana Trench is 1,550 mi. (2,500 km) long, but only a handful of spots, less than 30 mi. (50 km) long, are deeper than 32,800 ft. (10,000 m), including three in the Challenger Deep, one of which is the deepest place on Earth. The nearby continental plates are volcanic in nature and are known earthquake areas.

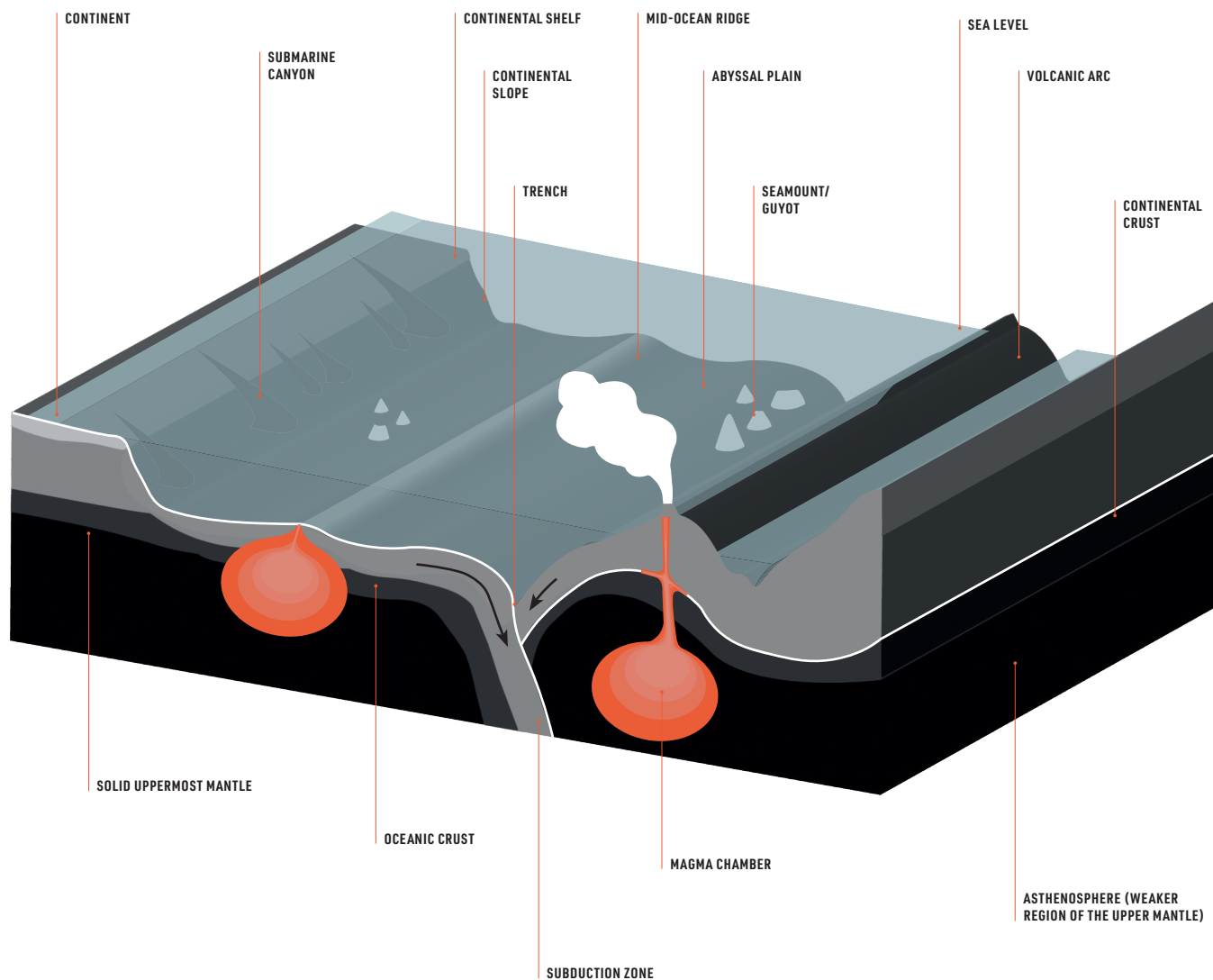
Abyssal plains

Shallower than the trenches, huge relatively flat seafloor areas are called abyssal plains. There, too, topography may show variability, in the form of abyssal hills and also isolated mountains. Such mountains can reach high up, even above the sea surface, forming islands. When such mountains remain under the surface, they are called seamounts, or guyots when their tops are flat. If they are part of a volcanic arc they may form hot spots of unusually warm and metal- and nutrient-rich waters.

All underwater topography is of importance for deep-sea life. In areas where minerals are spread into the ocean, waters are enriched, and particularly adapted life may thrive. Currents will redistribute the enriched waters. The topography also focuses deep-sea motions in various ways, and they may become so vigorous that turbulent mixing results (see pages 52–65).

Seafloor regions

The naming of various seafloor regions. All occur in the deep sea, except the continental shelf.



PROPERTIES OF SEAWATER

It's more than just water

Of course, ocean water is not just water. The average density of seawater at the surface is around $1,025 \text{ kg/m}^3$; this is more than 800 times denser than air (which has a density of 1.2 kg/m^3). Seawater is denser than fresh water (which has a density of $1,000 \text{ kg/m}^3$ at $39^\circ\text{F}/4^\circ\text{C}$) because the dissolved salts increase the mass by a larger proportion than their addition to volume. On average, seawater in the world's oceans has a salinity (the amount of dissolved inorganic matter) of about 3.5%. This used to be referred to as "35 per mil," or parts per thousand (ppt), but this is now considered a dimensionless number, as is "salinity of 35 g/kg ." This means that every kilogram (roughly about a liter by volume) of seawater contains approximately 35 g (7 teaspoons) of dissolved salts. The dominant dissolved ions are sodium (Na^+) and chloride (Cl^-), with smaller amounts of magnesium, sulfate, and calcium. In comparison, human blood has a salinity of about 9 g/kg . The freezing point of seawater decreases as the salt concentration increases. At typical salinity, freezing occurs at about 28.4°F (-2°C), the lowest temperature of liquid seawater.

Speed of sound

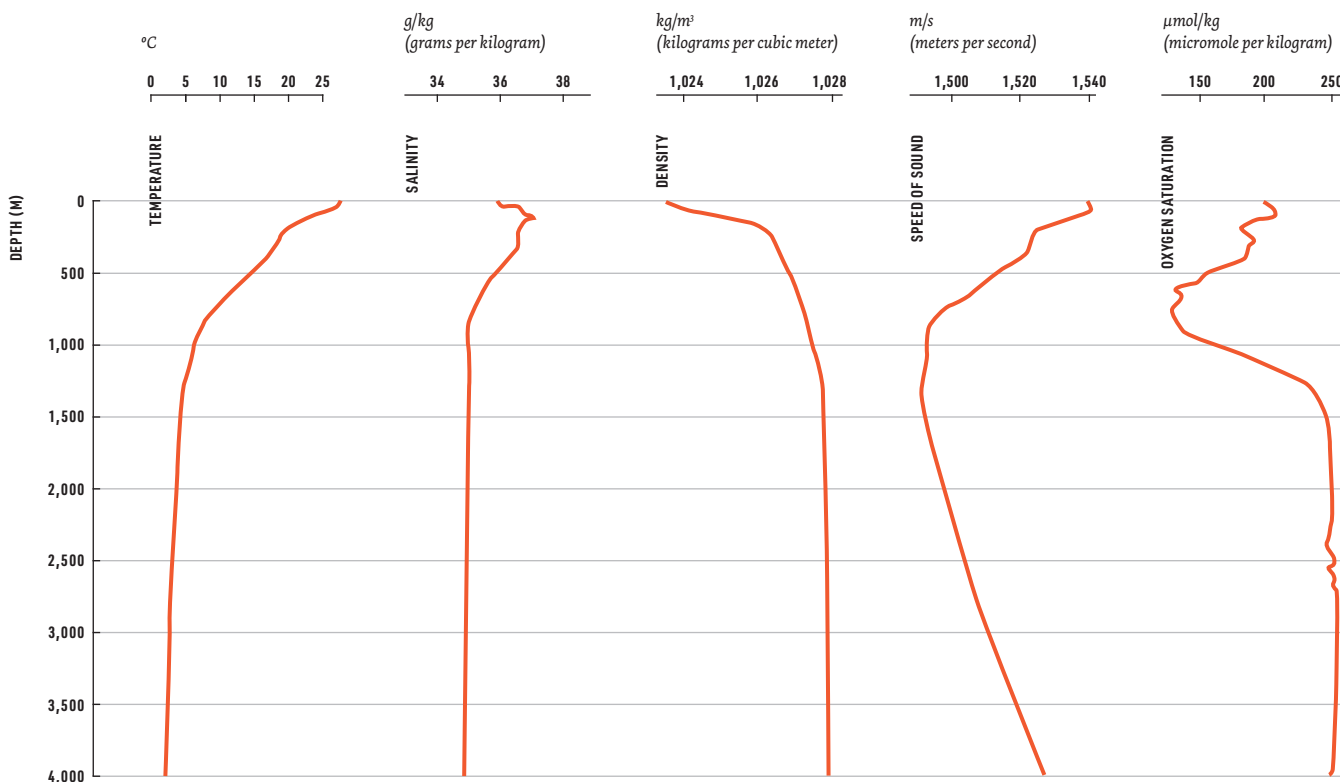
In the deep sea, values of different parameters may vary from their near-surface values. Temperature generally decreases with increasing depth, while salinity shows a more variable vertical profile in the deep sea, depending on the location. In general, most vertical density variations are caused by differences in temperature. After correction for slight, but nonnegligible, compressibility effects, density increases seemingly monotonically with depth—a monotonic trend is either only increasing or only decreasing. Speed of sound, however, is not a monotonic function of depth. Minimum speeds occur at intermediate depths, between about 3,280 and 4,290 ft. (1,000 and 1,500 m), because temperature, pressure, and salinity affect the speed of sound. Near the surface, temperature effects dominate, with lower speeds at lower temperatures, while deeper down pressure dominates, with higher speeds at higher pressure. This results in the SOFAR (sound fixing and ranging) channel of minimum sound speed at intermediate depths, causing sound waves to be retained within that depth range while propagating long distances. Low-frequency sound waves within the channel may travel thousands of kilometers before dissipating.

Oxygen saturation

Similar to the profile of sound speed with depth, oxygen saturation in the deep sea shows variation, reaching a minimum between about 1,640 and 4,920 ft. (500 and 1,500 m), depending on local physical and biological circumstances. This oxygen-minimum zone (OMZ) results from an interplay of relatively low turbulent mixing that limits supply of fresh oxygen from waters above and below and large oxygen consumption by bacteria feeding on organic matter raining down from the surface. The source of ocean oxygen is the exchange with atmospheric air. Most of the organic matter is decomposed in the upper 4,920 ft. (1,500 m), and oxygen saturation is relatively high in deeper waters due to low consumption.

Water properties

Depth profiles showing the temperature, salinity, density, speed of sound, and oxygen saturation in the Puerto Rico Trench in the western Atlantic Ocean.



Sound waves

Fin Whales (*Balaenoptera physalus*) are known to dive down to the SOFAR (sound fixing and ranging) channel of minimum sound speed at intermediate depths to communicate with other Fin Whales large distances away.

pH and salinity

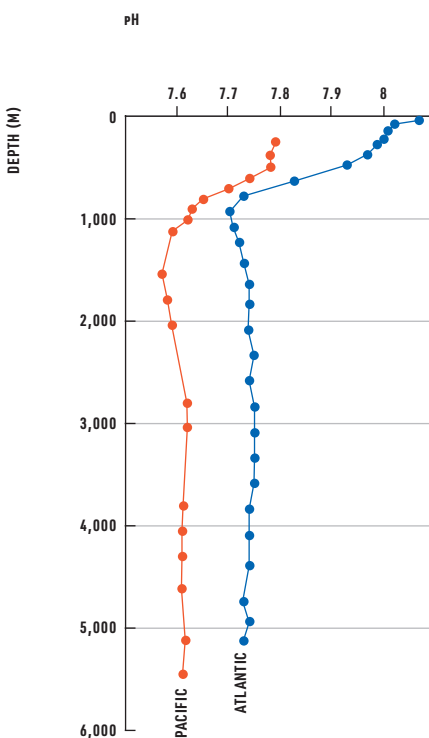
Seawater is basic (alkaline), as indicated by typical pH values are larger than 7, limited to a range between 7.6 and 8.2. Generally the higher (relatively more basic) values are found near the surface, and the lower (relatively more acidic) values are found in the deep sea, reaching minimum values around 3,280 ft. (1,000 m), a depth profile that is very similar to the deep-sea oxygen profile.

Ocean salinity has been stable for billions of years, most likely a consequence of a chemical/tectonic system that removes as much salt as is added. Seawater contains more dissolved inorganic matter than fresh water, and the ratios of solutes differ dramatically. For example, seawater contains about 2.8 times more bicarbonate than river water, governing pH and alkalinity in seawater. However, the percentage of bicarbonate in seawater as a ratio of all dissolved ions is far lower than it is in river water. Differences like these are due to the varying times that seawater solutes remain in solution; sodium and chloride have very long residence times, while calcium (vital for carbonate binding—i.e., shell building by marine animals) tends to precipitate much more quickly. Small amounts of other substances are found, including amino acids at concentrations of up to 2 micrograms of nitrogen atoms per kilogram, which are thought to have played a key role in the origin of life.

Microbial life

Seawater also contains abundant amounts of microbial life in the form of bacteria, archaea (single-celled prokaryotic microorganisms), and viruses. DNA research has revealed a great diversity in microbial life forms, to the extent that a bucket of seawater may hold more than 20,000 species. The world's oceans are thought to contain over 10 million species. Bacteria are found at all depths in the deep sea as well as in seafloor sediments; some are aerobic (consuming oxygen), others anaerobic (not requiring oxygen for growth). Most are free-swimming, but many exist within other organisms—for example, bioluminescent light-emitting bacteria. Cyanobacteria (blue-green algae) played an important role in the evolution of ocean processes, enabling the development of stromatolites (microbial reefs) and oxygen in the atmosphere. Some marine bacteria survive in a pH range of 7.3–10.6, while other species will grow only at pH 10.0–10.6, exceptional and unusually alkaline local conditions compared with general ocean waters.

Archaea, which also live in the deep sea, may constitute as much as half the ocean's biomass. These bacteria-like organisms survive in extreme environments, such as the hot and sulfurous hydrothermal volcanic vents on the seafloor. Studies of seafloor sediments have revealed archaea that break down methane as well as bacteria that break down seafloor rocks, thereby influencing seawater chemistry.



Deep ocean acidity

Ocean average profiles of pH as a function of depth. At all levels the Atlantic is less acid than the Pacific, because of shorter residence times of the water.

Bioluminescent bacteria

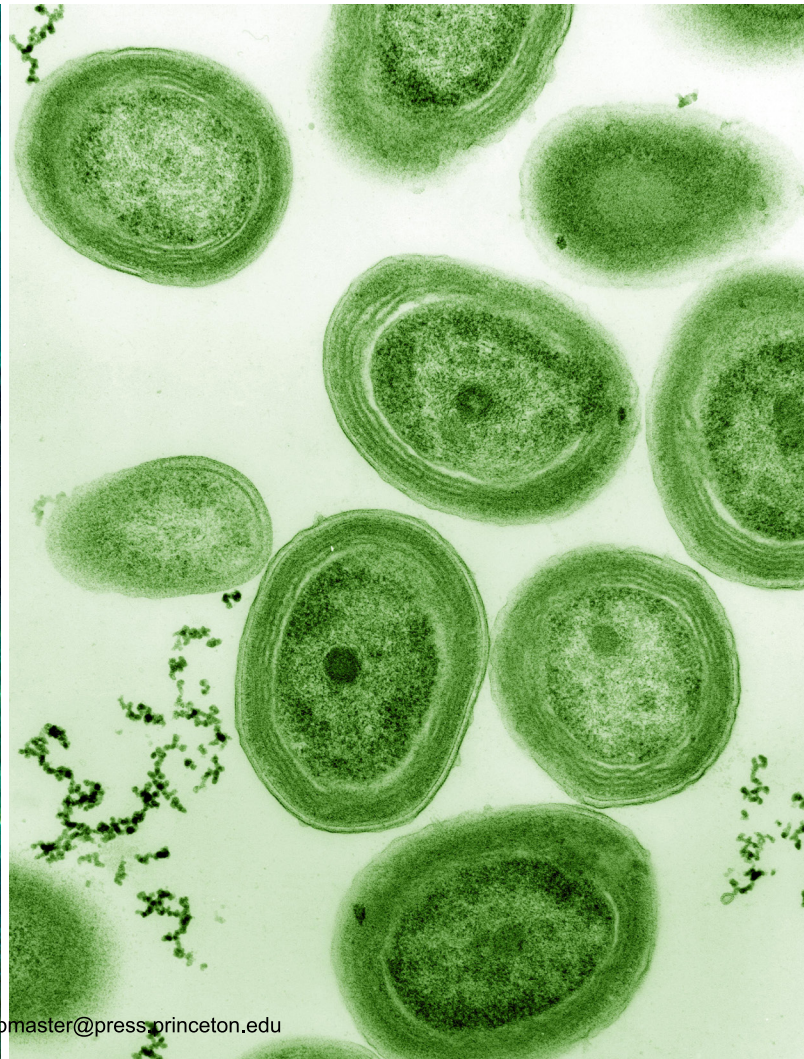
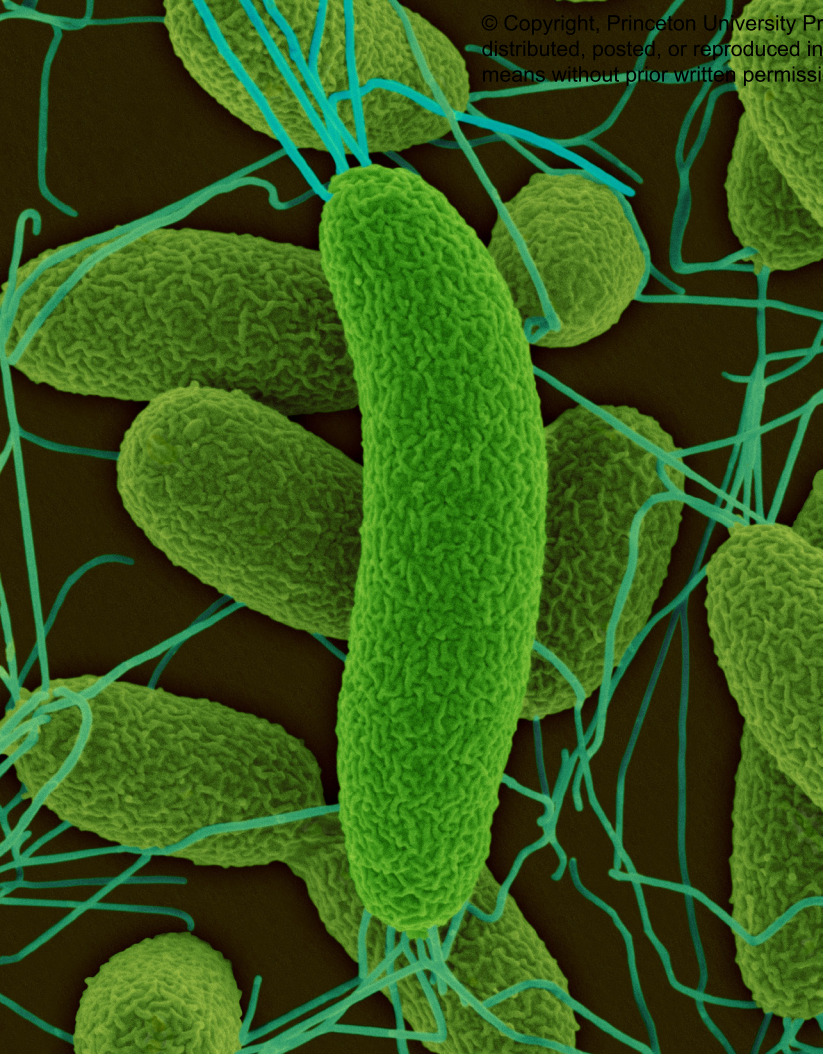
Top left: *Vibrio fischeri* is a bioluminescent bacterium that is found in many oceans around the world, working in a symbiotic relationship with certain deep-sea marine life.

Stromatolites

Bottom left: these microbial reef communities are formed from the precipitation of calcium carbonate by cyanobacteria.

Cyanobacteria

These single-celled organisms, which live in the deep sea, evolved to produce energy from sunlight and oxygenated the ocean. Top right: A micrograph of a diatom (oval) on cyanobacteria. Bottom right: A micrograph of *Prochlorococcus marinus*, a globally significant marine cyanobacterium



CURRENTS AND TURBULENCE

How ocean waters move

Water movements in the deep sea are not steady flows, but vary over multiple space and time scales. The spatial scales of variation range from ocean-basin scales for large flows of thousands of kilometers to millimeter scales for the smallest turbulence. The time scales vary between several hundreds of years of residence for ocean-basin flows, as determined from radiocarbon dating, to a hundredth of a second for turbulence-dissipation time scales. To date, measurement devices or numerical modeling capabilities have not been constructed to describe the dynamics of the deep sea at all scales. For example, large-scale ocean circulation models do not contain details of turbulent mixing processes. Whether quantifying these could ever be possible, given the complexity of intrinsic processes with various interactions between motions at different scales, is questionable. The dynamics of the ocean may prove to be inherently unpredictable and, until proven otherwise, they remain a mystery to solve, like the physics principles of turbulence. However, that does not preclude the study of limited-scale portions or specific dynamical processes in confined deep-sea basins.

On the large spatial scale, water motions in the deep sea follow those generated via the atmosphere near the sea surface, albeit commonly with smaller magnitudes. Westerlies, strong winds blowing from west to east around mid-latitudes in the Northern and Southern Hemispheres, drag water flows near the surface that eventually reach hundreds of meters into the deep sea. The winds are aided by equatorial trade winds blowing from east to west to set up gyres, large ocean-basin-scale circulations. Gyres consist of pressure-difference-driven flows that are intensified with the aid

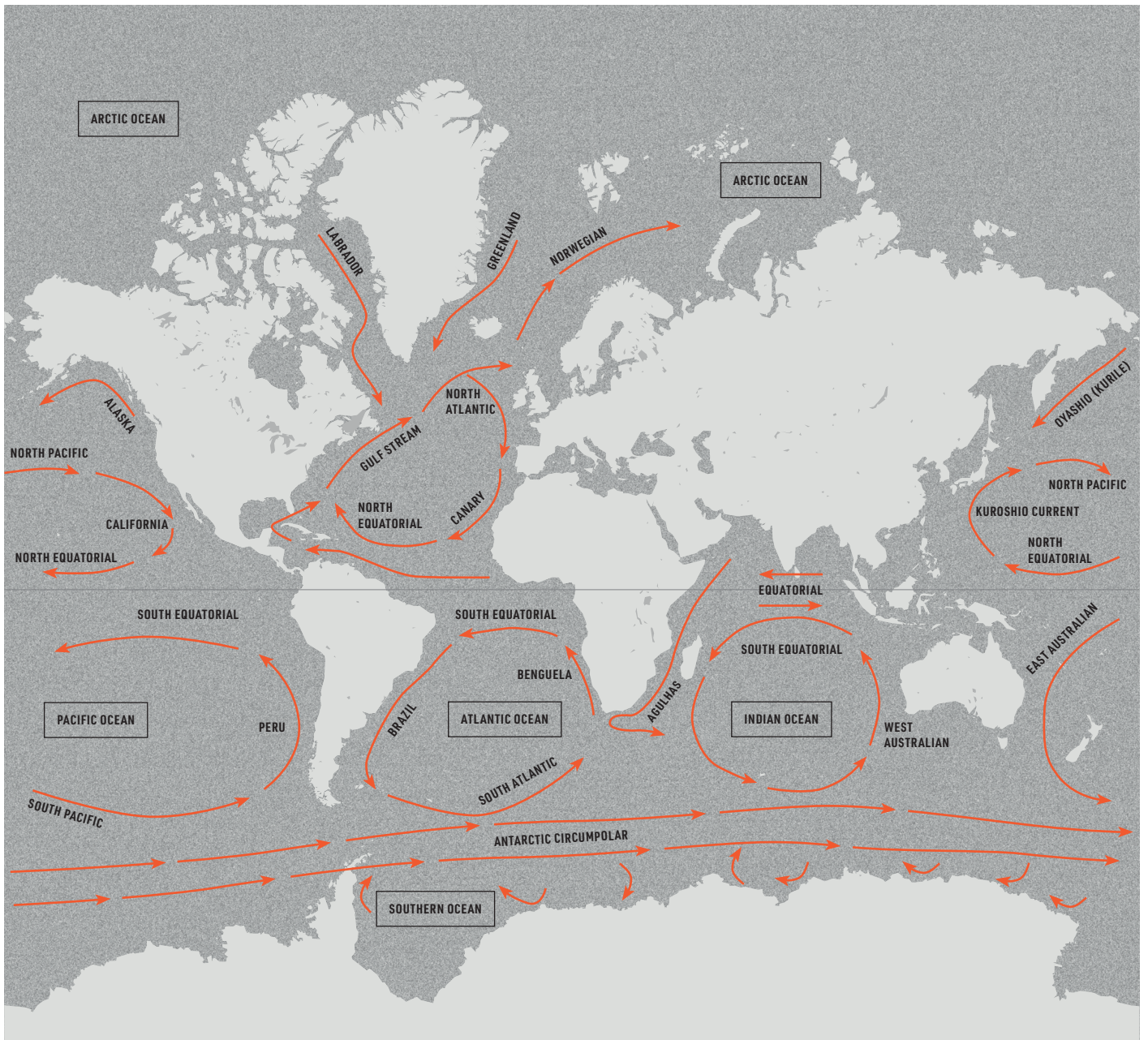
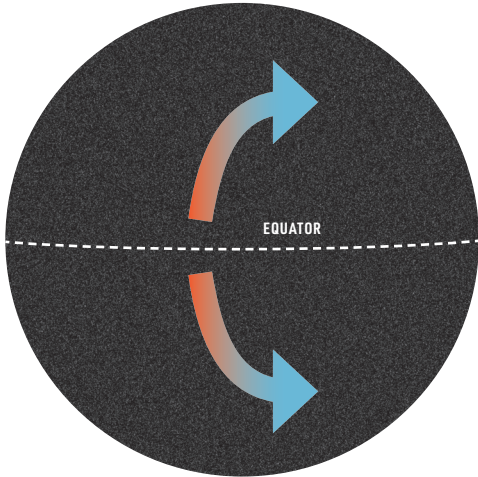
of the earth's rotation and steered by topography at the basin's western boundary. Examples of intensified wind-driven flows are the Agulhas Current in the Indian Ocean, the Kuroshio Current in the Pacific Ocean, and the Gulf Stream in the Atlantic Ocean. The world's largest flow (by volume of water transported) is the Antarctic Circumpolar Current, which is also mainly wind-driven. All these large-scale flows are diverted by the Coriolis effect, a pseudo-force resulting from the earth's rotation. In the Northern Hemisphere, a flow driven by a pressure difference is deflected to the right, up to the point that the Coriolis and pressure-difference forces balance and cancel each other out. Wind setup—winds blowing waters to pile up on one side—creates a surface pressure-difference force that is constant with depth. In the deep-sea interior, horizontal density differences (fronts) induce an independent pressure-difference force that varies with depth.

Coriolis effect

The Coriolis effect results in the deflection of major ocean currents to the right in the Northern Hemisphere and to the left in the Southern Hemisphere. The Coriolis force also results in major ocean spirals of ocean-circling currents called "gyres," directed clockwise in the Northern Hemisphere and counterclockwise in the Southern Hemisphere.

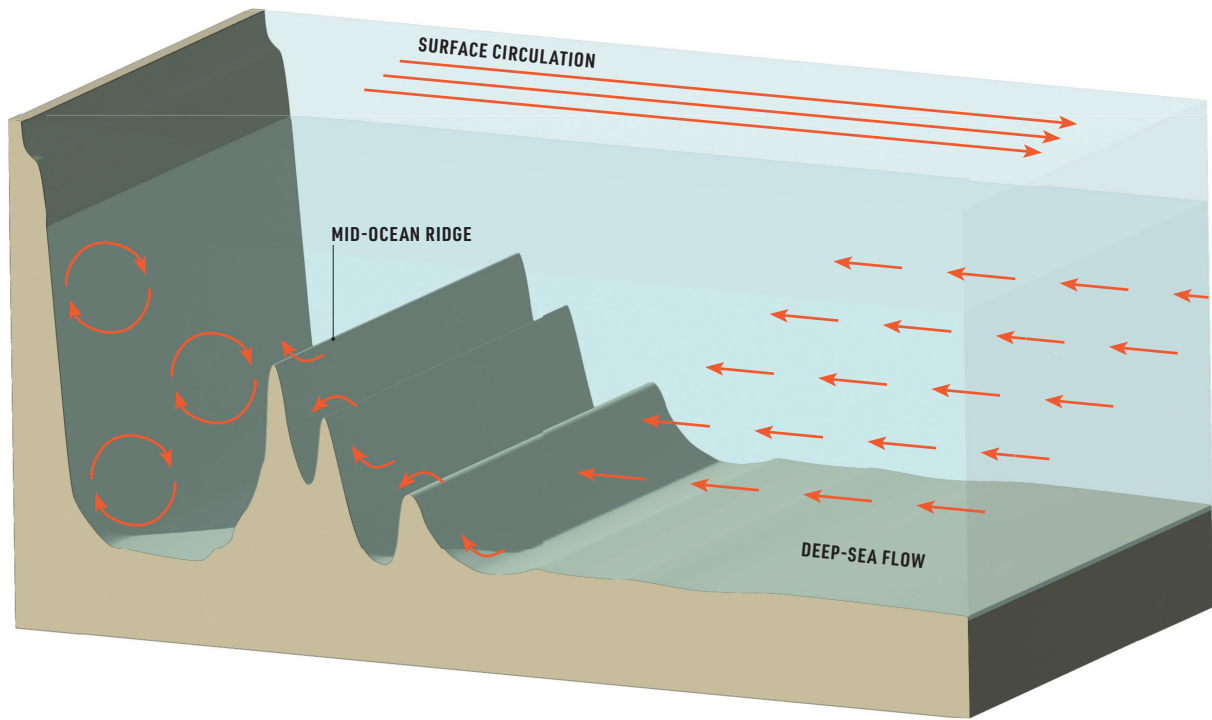
Ocean currents

The circulation on the ocean surface driven by westerly winds and the earth's rotation can reach deeper than 660 ft. (200 m).



Deep-sea flows

These flows can often be found in opposite directions to those near the surface. Deep-sea flows over underwater topography like seamounts and mid-ocean ridges generate turbulent mixing.

**Deep-sea flows and density**

The deep sea is generally stably stratified in density. While the less dense, warm, and relatively fresh waters are found mainly near the surface, some of the heat (and salt) is transported to greater depths. The deep sea is thus characterized by horizontal layers of constant density, of which the value steadily increases with depth, although at greater depths the pace of increase is less. When the density layers are not horizontal, they cause horizontal fronts. These horizontal density differences lead to pressure differences that vary with depth. The pressure differences result in water flow, which becomes directed along the front by the Coriolis effect. Examples of such density-driven flows on the large scale are along the boundaries of primarily wind-driven flows such as the Gulf Stream or Kuroshio Current. The Antarctic Circumpolar Current is accompanied by three large fronts, one of which is the polar front.

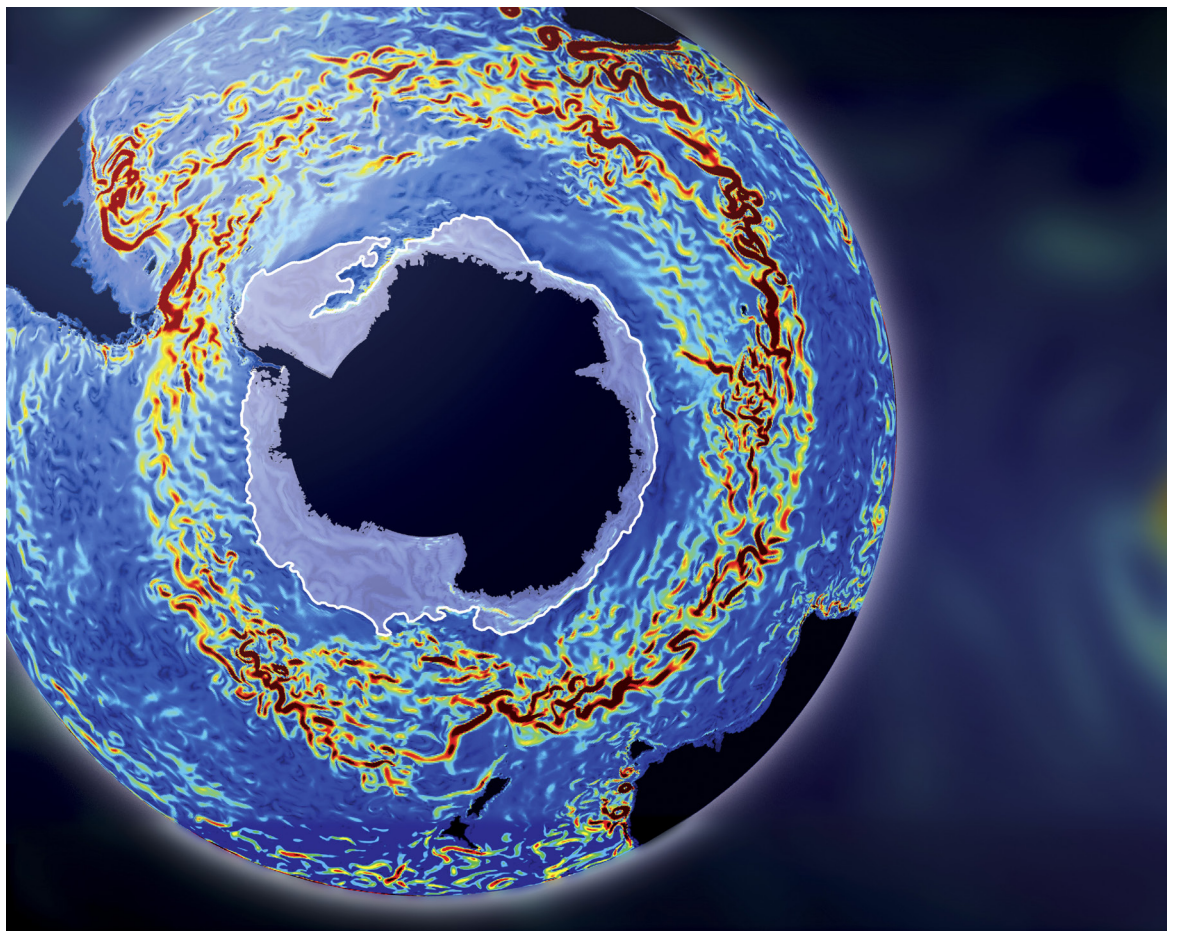
Although the large-scale, wind-driven flows are primarily in a balanced state, in which the pressure difference is balanced by the Coriolis effect, this does not mean that they are steady flows. Like the atmospheric winds, the flows show considerable variability in space and time. The flows are dynamically unstable; they maintain a steady direction, from which they repeatedly divert (or meander), like a river not flowing in a straight line. When the meandering becomes strong, the bend in the flow may pinch off to form an eddy, a circular movement of water causing a whirlpool, which can have a horizontal diameter of 60 mi. (100 km). The flow speed also varies, repeatedly, by more than two times. Large-scale flows thus give the impression of a strongly pulsed, variable phenomenon.

Large-scale flows driven by density differences are also found in the deep sea, where current flows are generally weaker than near the surface. These flows are intensified, and less attenuated, above topographic boundaries like continental slopes. Depending on the direction of the horizontal density difference, which may be different from the surface pressure difference, the deep-sea flows go in the opposite direction (as countercurrents) to the near-surface flows above. At depths greater than 3,280 ft. (1,000 m), such flows can still attain speeds of several tens of centimeters per second (0.1–0.2 m/s), up to ten times greater than flow speeds well away from topographic boundaries in the deep-sea interior.

Smaller topographic features than a continental slope may induce smaller-scale flows. Canyons incising a continental slope will deflect a boundary flow, which will be accelerated or decelerated accordingly. Submarine mountain chains like the Mid-Atlantic Ridge and the Central Indian Ridge are incised by numerous fracture zones, long and deep valleys between the ridge sections. Water flowing into the fracture zones will accelerate. As the fracture zones themselves are not flat, narrow basins, but also show variable topography with smaller-scale cross-channel ridges, the through-flow will be accelerated or decelerated during its passage. With the accelerations, more turbulent mixing with the overlying waters is generated. Although dense waters flowing over the seafloor are modified by the mixing and thus become less dense, the fracture zones are an important conduit for their passage between deep-sea basins (see pages 74–75).

Antarctic Circumpolar

A computer model of the flow around Antarctica. The flow shows numerous whirls and eddies. The most intense flow is colored red.

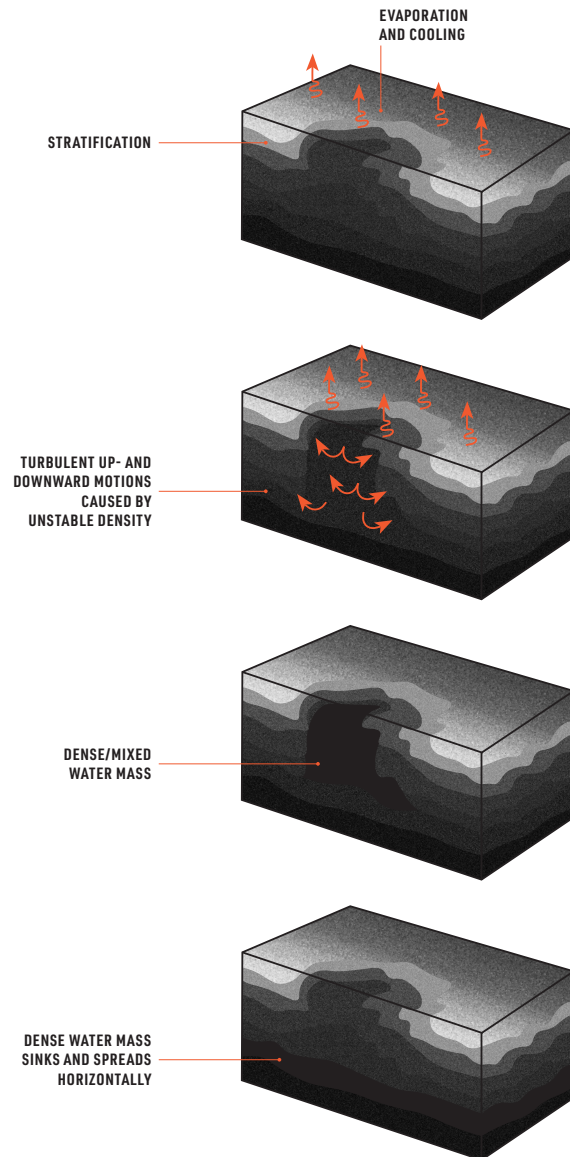


Density and the formation of water masses

Water masses are defined as large volumes of seawater that have distinctive properties, such as salinity, temperature, oxygen, or radio-isotope content, which each have values within particular bounds. Once formed, water masses will move away from the source, collide with other water masses, and eventually mix with them via turbulence processes. The deepest of these water masses, which also move and do not reside at a fixed spot, are denser than overlying water masses, consistent with stable vertical-density stratification in the deep sea. Deep, dense water masses newly form when the sea is unstably stratified in density, starting from the surface. This occurs only episodically, generally in localized areas near the poles as well as in a few mid-latitude sites in the Mediterranean Sea. Normally, in tropical, but also nearly all mid-latitude regions, near-surface density stratification by solar heating is so extensive that it strongly reduces turbulent mixing deeper than a few tens of meters. At greater depths, the stable stratification is thus not destroyed via instabilities by evaporation and nighttime cooling.

Under late-winter conditions in polar (and some Mediterranean) regions, however, overlying air may cool and evaporate sufficiently to result in relatively low temperature and high salinity content in near-surface waters compared to their deep-sea values. When the near-surface waters are cooler and/or saltier than waters below, the resulting unstable density stratification generates convective turbulent downward and upward motions, until reaching the depth level where the density values match those of the sinking waters. At their respective density level, the waters originating from the surface will spread into the deep interior by essentially horizontal transport.

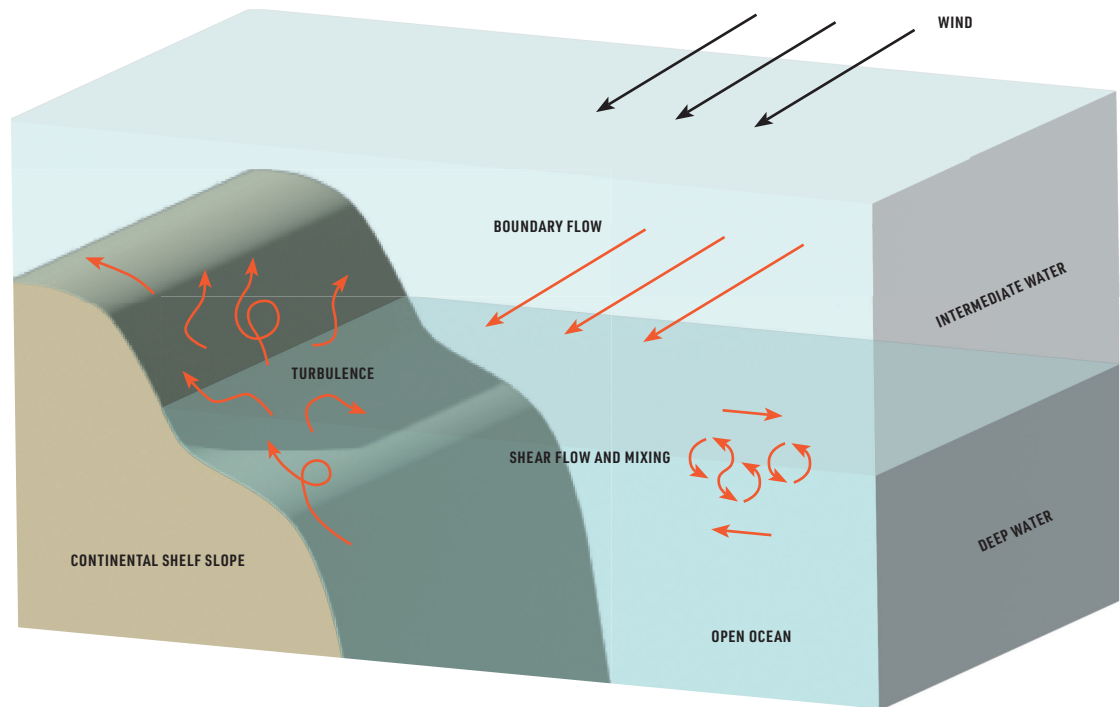
Once every 5–10 years, such sinking reaches seafloor deeper than 3,280 ft. (1,000 m), and the newly formed deep, dense water replaces the resident deep-water masses. The replacement is one way to set the deep water in motion, and there will be a frontal horizontal density difference with the previous deep-water masses. From their sources, such as areas near the poles, the episodically formed deep, dense water masses will flow in pulses toward the equator. During the sinking and the equatorward flow, they will slowly but surely mix with overlying waters, due to interior friction via turbulent shear flow of waters moving at different speeds and/or in opposite directions.



Dense water-mass formation

Schematic diagrams of deep convection. From above to below: preconditioning by evaporation and cooling, deep convection in narrow tubes, mixing, and horizontal spreading after sinking (after Marshall and Schott, 1999).

Mixing and turbulence
Open-ocean deep currents flow smoothly along constant density surfaces (isopycnals), where they mix via turbulence generated from flow-shear. Turbulent mixing by internal-wave breaking and boundary flows is 100–1,000 times more powerful above sloping topography than in the open ocean.



Deep-sea flow and mixing

Although the dense deep-water formation may invoke the image of a continuous large-scale, density-driven flow from polar to equatorial regions and beyond, the reality is different. The deep, dense water formation occurs in pulses, and so does the flow of dense waters over the deep-sea topography. Dense water formation varies not only on seasonal scales, but also on decadal scales, with the real deep formation occurring once in 5–10 years. Within the seasons, formation pulses vary from daily scales to shorter-than-hourly scales. The episodic pulses, varying on so many scales, do not continuously cause a deep-sea river or conveyor belt. Envisioning the deep-sea flow using such metaphors may be tempting but does not correspond with the dynamical processes of the ocean.

Once a dense water mass is formed, its spread along the seafloor or, when not reaching to the seafloor, along layers of constant density (isopycnals), smooths the pulses somewhat. The smoothing is governed by interior slow, turbulent mixing processes, which may become stronger when the flow of interacting layers occurs at different speeds or directions (shear), resulting in friction and turbulent mixing. Thus, the denser waters near the deep seafloor will gradually become less dense during their transport equatorward (and overlying waters gradually denser). No matter how slow the modification, as water masses can be traced for decades, this interior exchange via turbulent mixing is still about 10–100 times faster than molecular exchange would be in a nonturbulent flow. More energetic, and thus faster, turbulent mixing occurs in some regions of the deep sea.

In the open ocean, the shear- and/or internal-wave-induced turbulent mixing is about 10 times more intense near a flat seafloor of a deep basin than turbulent mixing away from the bottom. Turbulent mixing is 100–1,000 times more powerful in a layer about 330–660 ft. (100–200 m) thick above sloping topography than in the open water column. We already noted the accelerating flows over small-scale topography in fracture zones of a mid-ocean ridge, but the largest turbulent mixing in the deep sea occurs via the breaking of internal waves. Such waves are ubiquitous in the density-stratified deep sea, as we elaborate next. All the turbulent mixing that touches the seafloor whirls up sediments, which are subsequently transported by the larger-scale flows. Outside the polar regions, all the turbulent mixing also ensures that the ocean is stratified by the heat transfer from surface to bottom, thereby compensating for the potential energy loss due to the sinking of newly formed dense—cold and salty—water. Without turbulent mixing, the deep ocean would become a stagnant pool of cold water, not driven at all by differences in density.

Due to their large scales, flows in the deep sea are turbulent everywhere and a laminar- (or smooth-) flow environment does not exist, except at the level (smaller than 0.5 in./1 cm) of water flowing past a very small swimming animal.



Going with the flow

Clockwise from top left: *Porphyrocrinus* sea lily, American Samoa; brown cerianthid tube anemone, Gulf of Mexico; *Relicanthus* sp., a new species from a new order of Cnidaria, Clarion-Clipperton Fracture Zone, eastern Pacific; large stalked anemone, Gulf of Mexico.

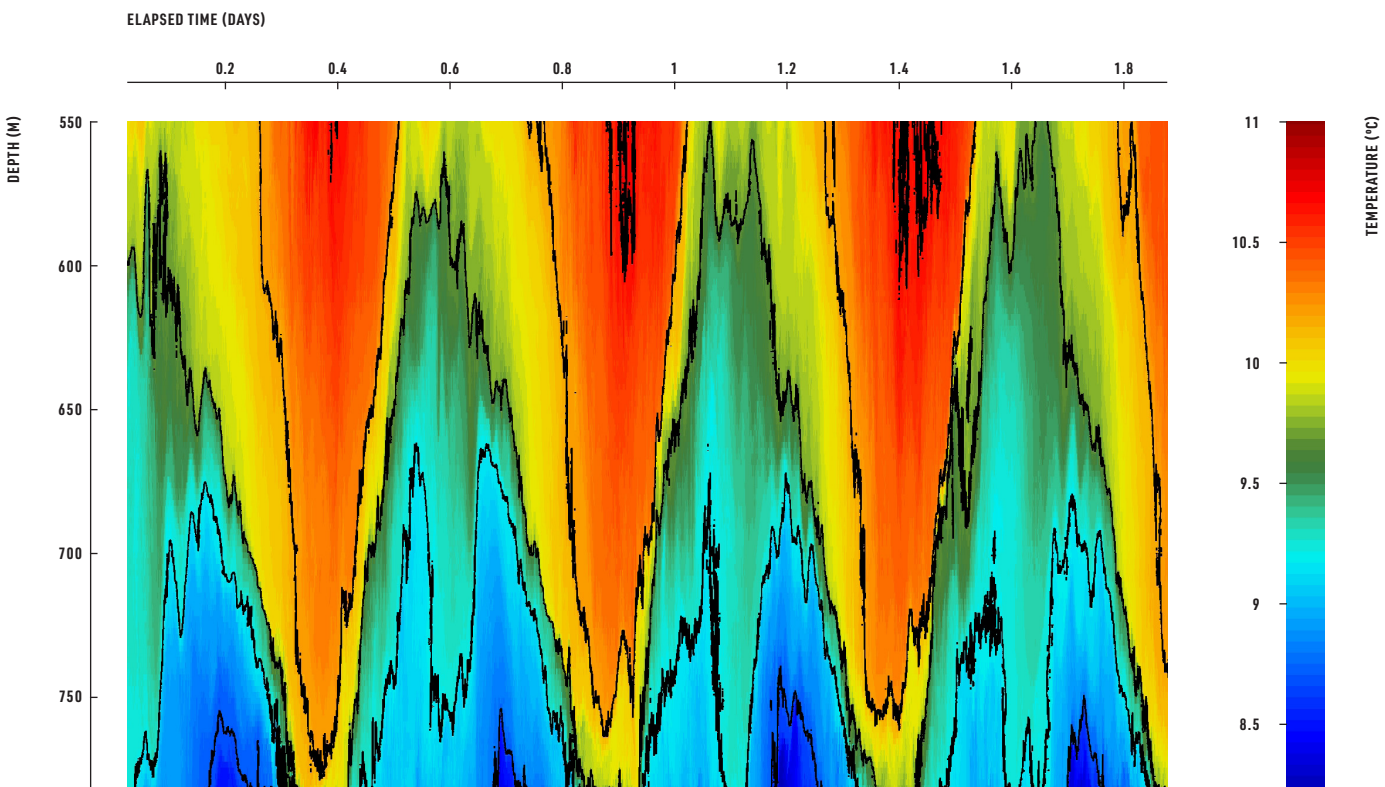


Tides, wind, and internal waves

A major source of turbulence in the deep sea is related to tides, the gravitational pull of the moon and sun on ocean water. If a current meter is held anywhere in the deep sea for some time, it will measure kinetic energy, the energy of motion. A spectrum—a graph displaying energy levels as a function of time—will generally show the largest peaks at (1) semidiurnal and (2) inertial frequencies. This implies that most energetic motions are related to (1) the tide—dominant semidiurnal variation shows tidal peaks that occur twice a day; and (2) the rotation of the earth, with the Coriolis effect resulting in an inertial motion with an oscillation frequency of about one day, depending on the latitude. These motions contain about 1–2 TW (terawatts) and 0.5–1.0 TW of energy, respectively, globally—more kinetic energy than the other large-scale flows in most of the deep sea. Such values may be compared with 16 TW in present consumption by humankind, about 2,000 TW of ocean heat transport, and roughly the same, or more, of atmospheric heat transport, and about 120,000 TW of solar radiation reaching the ocean surface.

Whittard Canyon internal tide

A 660 ft. (200 m) from-crest-to-trough tall internal tide detected by temperature sensors at Whittard Canyon in the northeast Atlantic. The graphic shows the peaks and troughs. Map shows location of Whittard Canyon, highlighted with the red circle.



Why would the small amounts of ocean kinetic energy in tidal and inertial motions, compared with the huge amounts of heat transport, be important for deep-sea turbulence and, thereby, for deep-sea circulation? The two main kinetic energy peaks have different sources. The semidiurnal peak has its source in the surface pressure difference following the earth–moon (and sun) interaction. In the deep sea, the resulting relatively weak horizontal tidal motions may induce a vertical motion when they encounter underwater topography. The vertical tidal motion will displace horizontal density layers, which thereby create internal waves with tidal frequency.

As the vertical density differences are relatively weak in the deep sea, typically less than one one-thousandth of the density difference between air and water, internal waves are different from sea-surface waves. Internal-wave amplitudes can reach over 330 ft. (100 m) vertically, while they go nearly unnoticed at the sea surface, displacing only 4 in. (10 cm). Their typical wavelengths (the distance from peak to peak) are in the order of 0.6–6.2 mi. (1–10 km), while surface tides can have wavelengths of thousands of kilometers. Internal tidal-flow speeds can grow up to several tens of centimeters per second in the deep sea, whereas surface tidal flows reach only 0.4–0.8 in./s (1–2 cm/s) in the deep. Internal waves travel slowly, at speeds of typically 4–39 in./s (0.1–1.0 m/s), compared with speeds up to several hundred meters per second for ocean-surface tidal highs and lows. Even at their most rapid frequency, internal waves are still slow waves, having typical periods of an hour or more in the deep sea, compared to sea-surface wind waves typically having 10-second periods. The lowest-frequency internal waves, those with the longest period, have a period of typically a day, depending on the latitude of generation. Any moving disturbance over and in a fluid on a rotating sphere will leave behind inertial motions—transient motions that are deflected by the Coriolis effect. Think of an atmospheric storm passing over the sea or a density front collapsing in the deep sea. The inertial motions left behind by such passing disturbances will set up internal waves that move near horizontally. The larger their vertical component, the deeper they extend into the deep sea, where stratification will be weaker.

Internal-wave breaking

Internal waves keep the stably stratified deep-sea interior in permanent motion, everywhere. When waves are moving freely in the interior, very little wave breaking may occur. However, throughout the deep-sea interior, internal waves of different frequencies and originating from different sources may locally enhance their energy when the waves interact. The smooth waves may then deform and become unstable. When they pass through layers of different currents above and below, undergoing vertical shear, the deformation may grow to the point of breaking. Shear is found, for example, in localized large-scale current systems, like the Kuroshio or the Antarctic Circumpolar Current, which weaken and thus shear at greater depths. Shear occurs in other areas, such as density-driven flows down a canyon, as well as in internal waves.

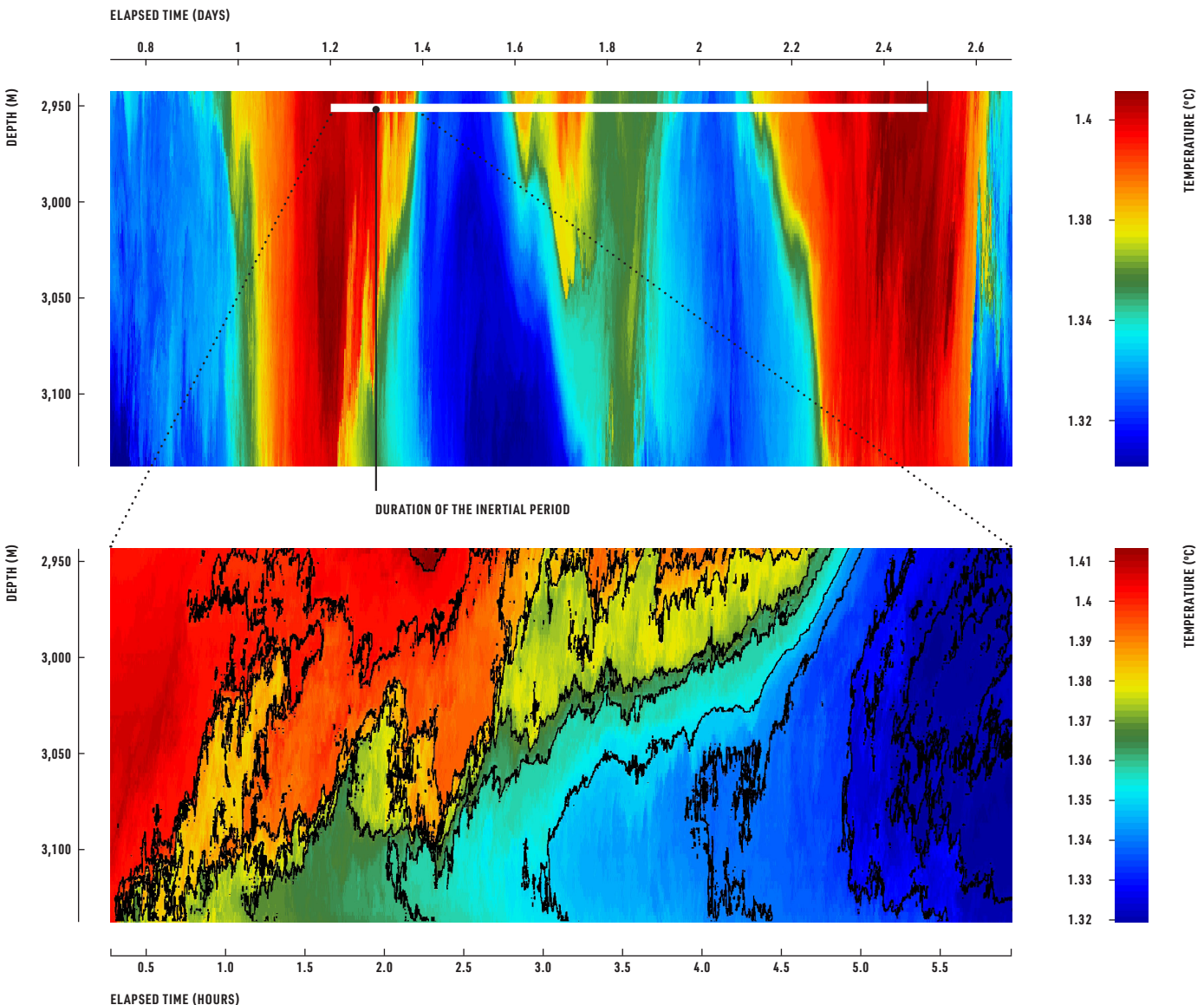
Paradoxically, the internal-wave shear destabilizes the density stratification, so that internal waves apparently destroy their own support via generation of shear. Although turbulent, this mixing occurs sporadically, intermittently, in the deep-sea interior, with a puff here and a puff there. Internal-wave turbulence can become more than 1,000 times stronger than this interior turbulence in localized spots of the deep sea above sloping underwater topography.

Slope characteristics

Like surface waves breaking on a beach, internal waves can break above underwater topography depending on slope characteristics of both topography and internal waves. By propagating in three dimensions under water, internal waves will encounter the boundaries of a basin. For example, large inertial waves generated by a typhoon (hurricane) in the northwest Pacific caused turbulent breaking 660 ft. (200 m) tall at 9,840 ft. (3,000 m) depth on the continental slope, amid slightly smaller internal tides colliding with the topography. Upon such an encounter with sloping deep-sea topography, internal-wave energy accumulates, and the overgrowing internal waves must break into turbulent mixing. In practice, such spots are not fixed in space and time but vary, because breaking occurs where the slope of the internal wave matches the slope of the seafloor, and because the slope of internal waves depends on local water stratification, which varies in space and time.

Turbulent breaking on a continental slope

Large inertial waves generated by a typhoon in the northwest Pacific caused turbulent breaking 660 ft. (200 m) tall at 9,840 ft. (3,000 m) depth on the continental slope, amid slightly smaller internal tides colliding with the topography. The white bar indicates the duration of the inertial period (about 1.25 days). The dotted line indicates the lower detail image of the internal wave breaking.

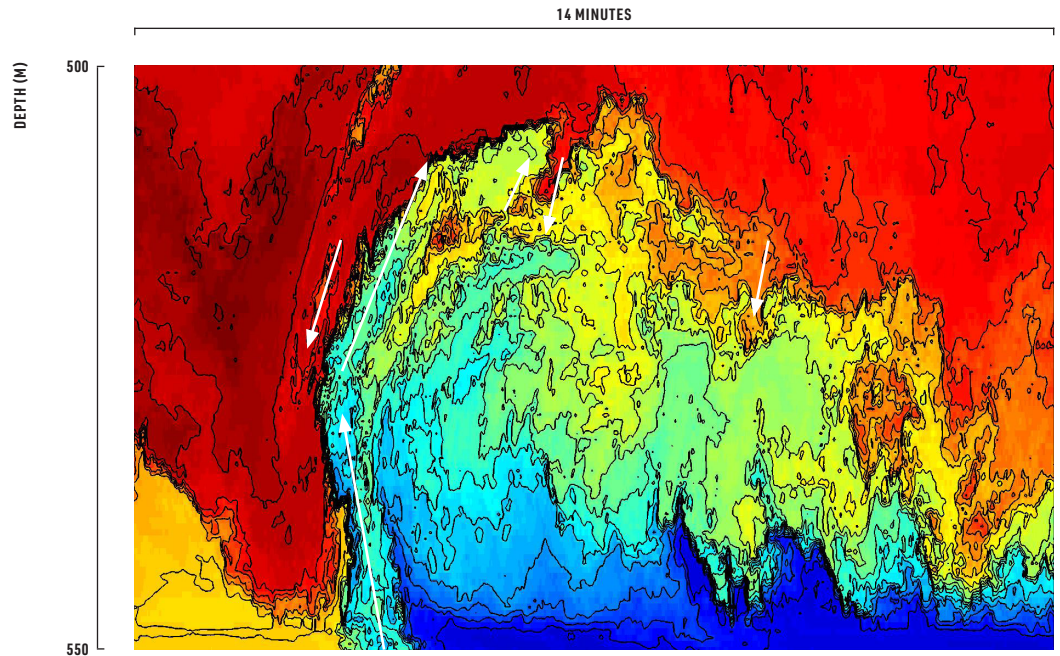


Backward-breaking internal wave

A large backward-breaking internal wave of an upslope moving solibore observed using temperature sensors near the top of Great Meteor Seamount, North Atlantic Ocean. The temperature ranges from 54.14 °F/12.3 °C (blue) to 57.38 °F/14.1 °C (red). The arrows roughly indicate the direction of motions. For example, around the strong front (change in temperature) the warm water is moving downward and the cold water upward at speeds of up to 6 in./s (15 cm/s).



ELAPSED TIME



Vigorous turbulence

Above topographic slopes, turbulent mixing and varying boundary-current flows alter the local stratification and thus the internal-wave slope at a particular frequency. As a result, internal-wave turbulent mixing also occurs episodically, mostly at topographic slopes that are just steeper (supercritical) than those of the prevailing internal waves. At times when conditions are right, the turbulence can be vigorous and spectacular, resulting in upslope-moving turbulent bores, or solibores—the steep leading edges of a traveling wave of water. Such bores of several tens of meters high have been observed in the deep sea. The impact of such vigorous events occurring a few times per (tidal) wave period on the seafloor fauna is large: sediments and nutrients are brought into suspension by vertical motions of more than 4 in./s (10 cm/s) up to 330 ft. (100 m) from the seafloor and are subsequently transported into the deep-sea interior. If one were at such a site, the event would feel like the passage of a Sahara dust storm, albeit underwater, in the pitch black of the deep sea.

Various observations have indicated that internal-wave breaking above topography is sufficiently strong in turbulent mixing to maintain vertical heat transport in the deep sea, thereby affecting the density stratification and thus the entire density-driven circulation of the ocean. An important property herein is that internal-wave breaking over sloping topography is very efficient. The back-and-forth sloshing of internal waves over a slope rapidly restratifies waters that are just mixed or homogenized. Homogeneous waters have a mixing efficiency equal to zero. Internal waves replace the mixed waters with stratified waters, which results in an efficient mixing property.

Turbulence over ridges and in trenches

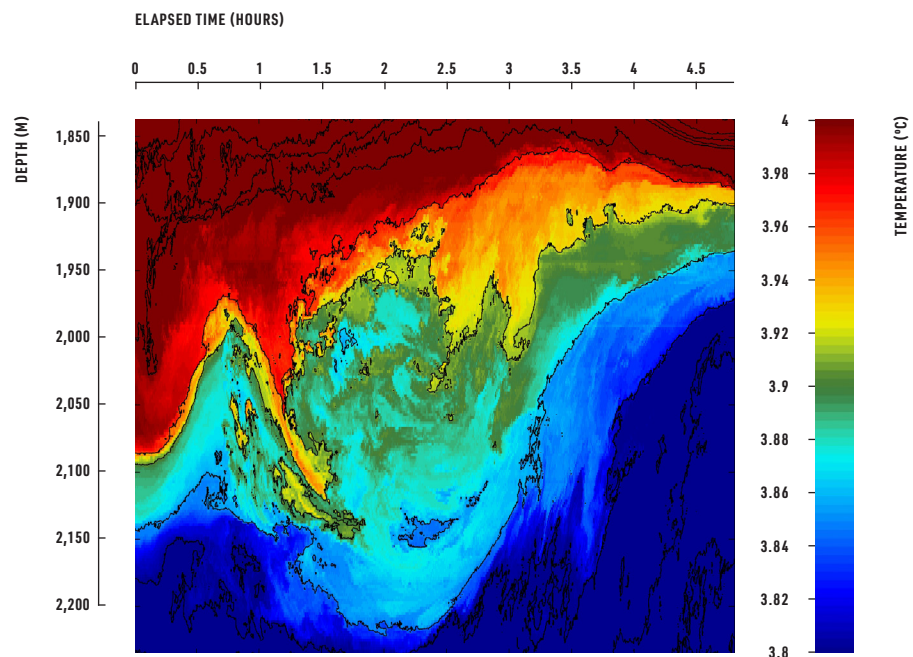
Strong and efficient turbulent mixing in the deep sea can also be found when internal-wave motions pass over small ridges. Depending on wave phase, the flow may become critical when the particle tidal-flow speed exceeds the phase speed of the wave, and the internal-wave crest topples over its trough. Convective overturning into wave breaking results, which can be pictured as a deep-sea washing machine—one 330 ft. (100 m) in height. Such internal action—known as hydraulic-jump mixing—generally does not touch the seafloor, but merely affects the water column directly above the ridge. It is therefore important for further transport of heat and suspended matter into the deep-sea interior.

Thus, although internal waves of several tens of meters in amplitude move suspended matter and nutrients up and down regularly during their propagation, it is the turbulence they induce that actually mixes these suspensions, which eventually become transported by large-scale current flows along isopycnals. Transport along isopycnals is much easier than across them, also in the deep sea where density differences between water layers are slight and little force is required to cause turbulent mixing between them.

The deeper one gets into the sea, the weaker the vertical density stratification and thus the weaker the restoring force of internal waves (gravity). As a result, internal waves attain a more vertical path of propagation, and their amplitudes can grow larger. The weakest stratification is expected to be found in deep-sea trenches. Nevertheless, rare observations demonstrate that turbulence here is not negligible, being about twice as powerful as that in the surrounding deep ocean. This may explain why the carbon flux into trenches is approximately twice as large as that found outside of trenches. While stratification is weak, the nearness of topography, because the side walls of trenches are relatively nearby, may focus internal-wave breaking into puffs, shooting here and there into the deep trenches. Deep-trench turbulent puffs are observed to occur more vertically and more often than in the surrounding deep ocean. Turbulence in trenches is observed to be generated not as much by current shear as by more of a convective-type motion, with episodic vertical shots of denser and less dense waters into the relatively quiescent surroundings.

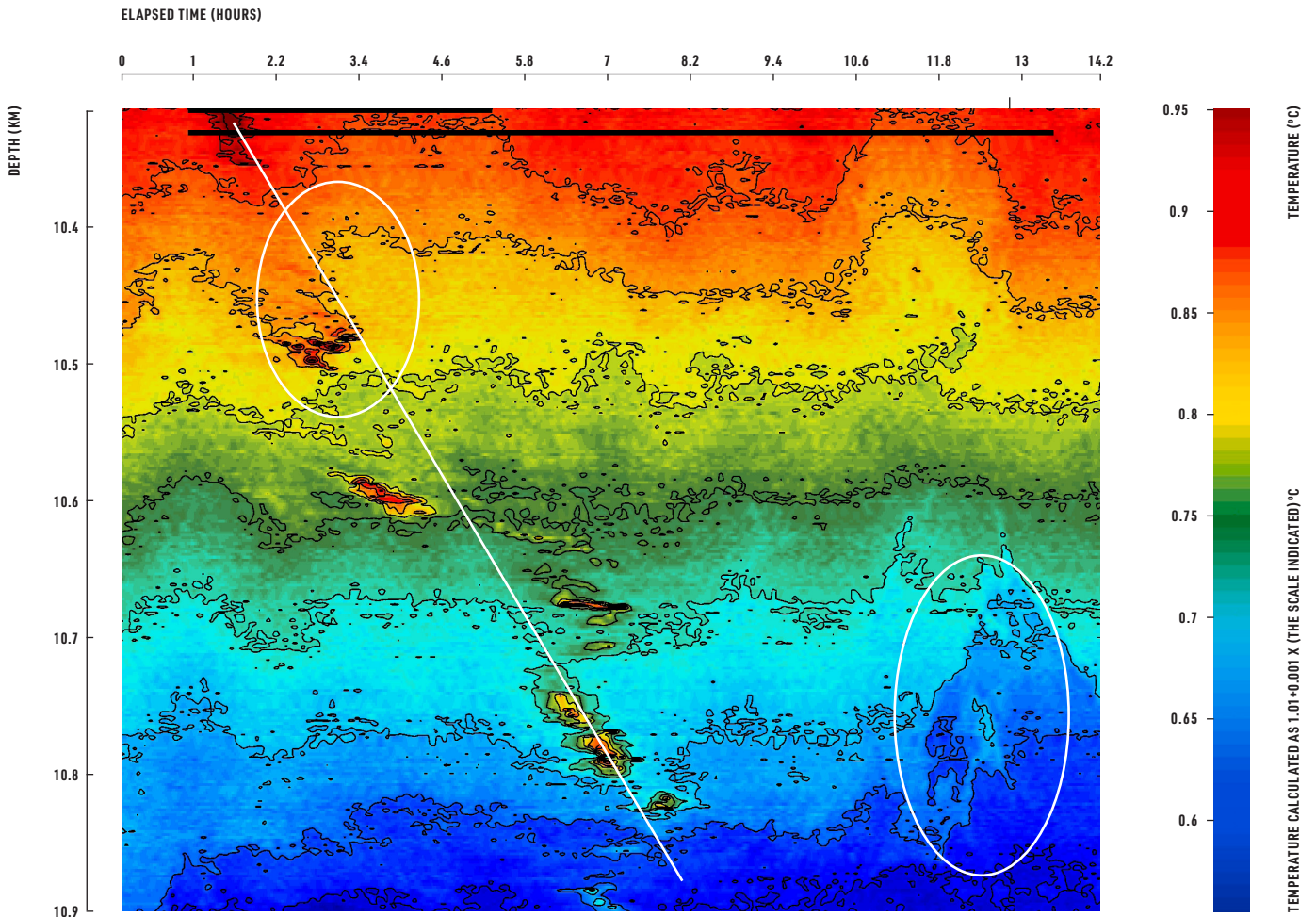
Hydraulic-jump mixing

A “washing machine” turbulent overturn over the Mid-Atlantic Ridge. The graphic shows data detected by high-resolution temperature sensors.



Mariana Trench turbulent jet

Occasional internal-wave breaking appears as puffs approaching the trench floor, as detected by temperature sensors. The white circles highlight relatively strong turbulent “puffs”; the white line indicates the direction of the turbulent puffs going down to the trench floor.



DEEP-SEA BASIN CHARACTERISTICS

The topographic basins that contain oceans and seas

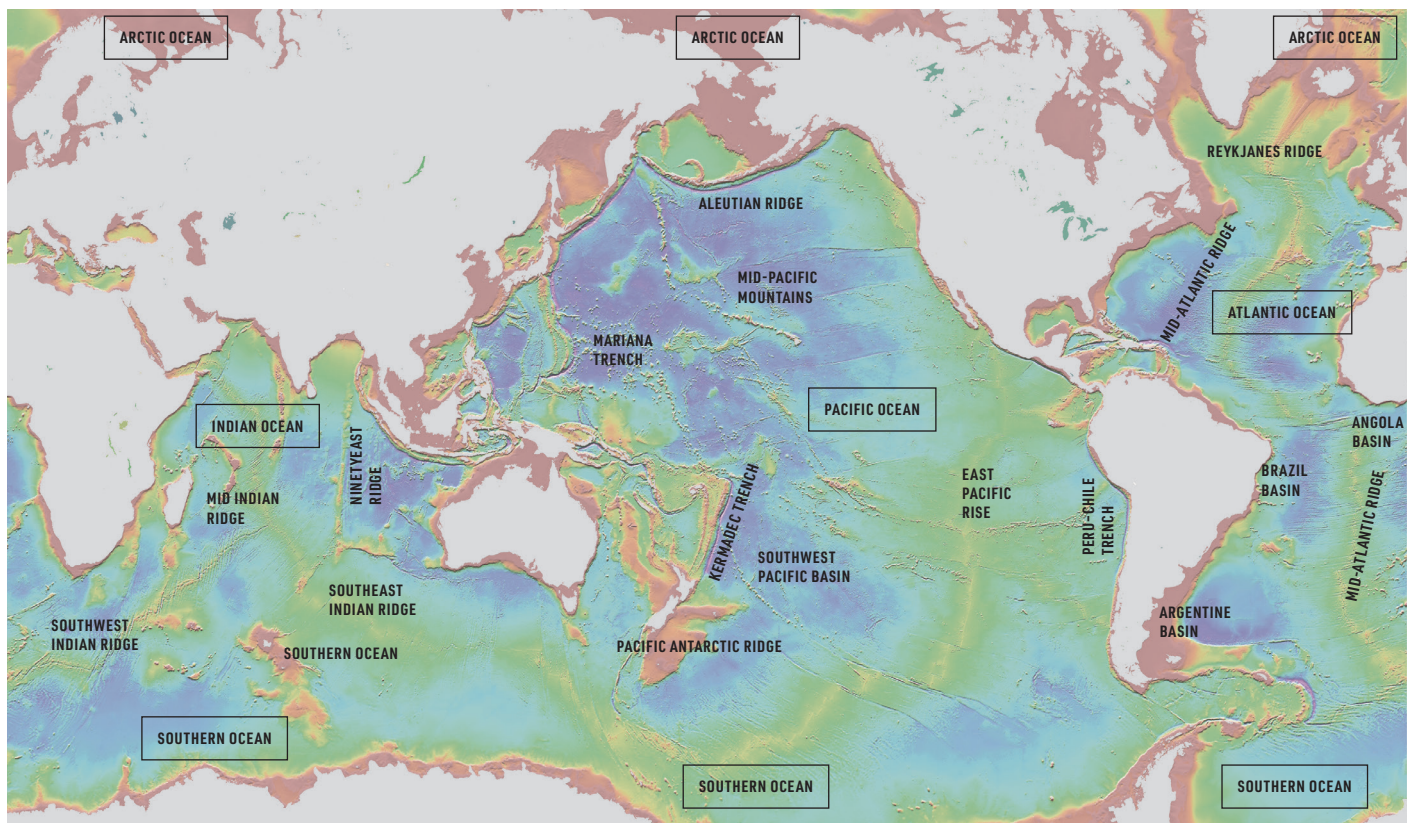
Deep-sea basins are areas in the ocean that are partially, or entirely, closed off by topography from other areas. Often, a deep-sea basin has a relatively flat floor surrounded by higher underwater topography like seamount ridges, continental slopes, or continents. Or a basin may feature a stirring of waters around isolated seamounts or islands in an otherwise dull, flat deep seafloor. Basins include large ocean basins and small, marginal seas. These may differ in size and in particular topographic features, but their characteristics and most of the overall dynamics are similar. Some basins can have exchange with other nearby basins, via sea straits or over underwater ridges. Those that do not can have different circulation and physical characteristics because of the limited exchange with other basins.

Ocean basins

Ocean basins are the largest water basins on Earth. Meridional cross sections of all ocean basins demonstrate large oxygen content near the surface, modest to large oxygen content from the seafloor upward, and extended oxygen-minimum zones (OMZs) between 1,640 and 4,920 ft. (500 and 1,500 m), of which the intensity varies geographically. In all basins, turbulence in the interior is at a minimum around 3,280–6,560 ft. (1,000–2,000 m) depth, while larger wind-induced mixing occurs near the surface and internal-wave breaking induces more turbulence over sloping topography.

Major ocean basins

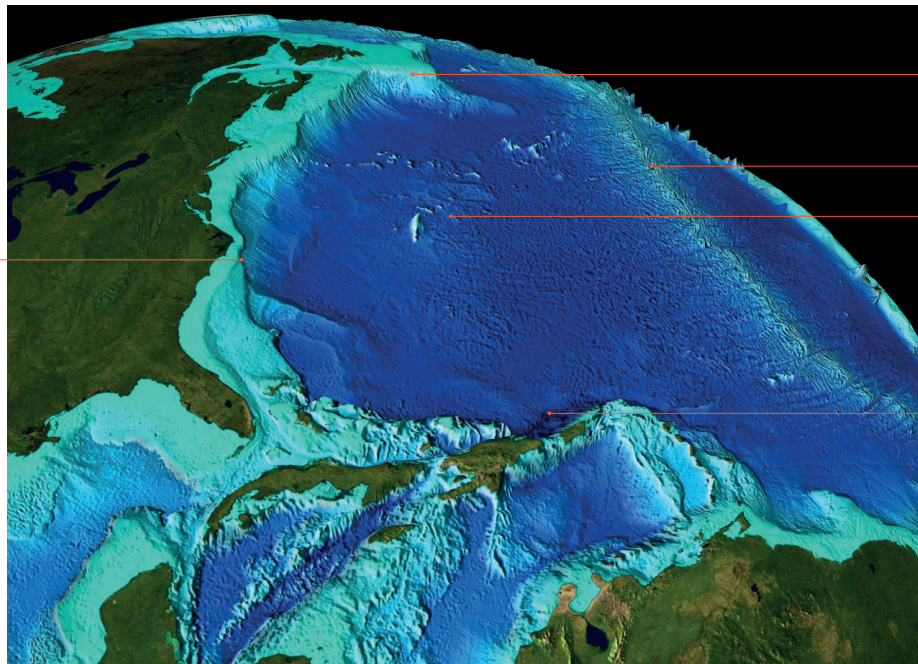
The five ocean basins include numerous subbasins that are separated, for example, via major underwater mountain ridges.



Atlantic Ocean basin

Large features are the drop down from the continental shelf to the abyssal plain and the Mid-Atlantic Ridge. Numerous small hills and mounts are also visible.

CONTINENTAL SHELF



GRAND BANKS OF NEWFOUNDLAND

MID-ATLANTIC RIDGE

BERMUDA

PUERTO RICO TRENCH

Atlantic and Pacific Ocean basins

While ocean basins and smaller sea basins have many similarities, a few characteristics unique to ocean basins can be named. The Atlantic Ocean is the only ocean that sees deep, dense water formation on both its southern and northern boundaries. The Indian Ocean, and notably the Pacific Ocean, see deep, dense water formation flowing in only from the southern side.

In its northern reaches, the present-day Pacific Ocean is almost blocked off from the Arctic Ocean by the Bering Strait. It has limited openings in the Aleutian Ridge to the Bering Sea, and its own surface circulation does not allow for sufficient cooling and, especially, evaporation to form deep, dense waters. The North Pacific demonstrates a much stronger salinity contribution to near-surface density stratification. Its near-surface salinity is about 32.8 g/kg, while its salinity deeper down is about 34.6 g/kg. For comparison, these values in the North Atlantic are 34.7 g/kg and 34.9 g/kg, respectively. Oxygen-rich dense waters are not uniformly found in the North Pacific, and the OMZ is larger and stronger there than in, for example, the North Atlantic.

While the Mid-Atlantic Ridge forms a seamount chain bisecting the entire basin from south to north, the North Pacific lacks a mid-ocean ridge. Deep flow, spreading and mixing through fracture zones from eastern to western basins in the Atlantic, hardly occurs in the North Pacific. However, the equatorial flow system, of strong east-west flows occurring between 10°S and 10°N, is more or less similar for Atlantic and Pacific basins. This flow system includes sharp contrast between westward and eastward flows near the surface, and counter-flows in various layers in the deep sea.

Indian and Southern Ocean basins

Because the Indian Ocean has limited extent north of the equator, its principal basin-wide gyre is found south of the equator. It thus has a very asymmetric appearance to its large-scale circulations, compared to those of the Atlantic and Pacific Oceans. Some of the world's warmest surface waters are found in its small northern part, which is blocked off by the South Asian subcontinent. A unique flow system with effects in the deep sea is the Agulhas Current, which is part of the large southern Indian Ocean gyre and transports warm waters near the surface and into the deep sea along the east African coast. It is the largest wind-driven flow after the Antarctic Circumpolar Current. The Agulhas Current splits off mesoscale eddies—eddies that have a diameter of about 60 mi. (100 km)—and collides heavily with Atlantic Ocean waters south of Africa, then turns to follow the Antarctic Circumpolar Current.

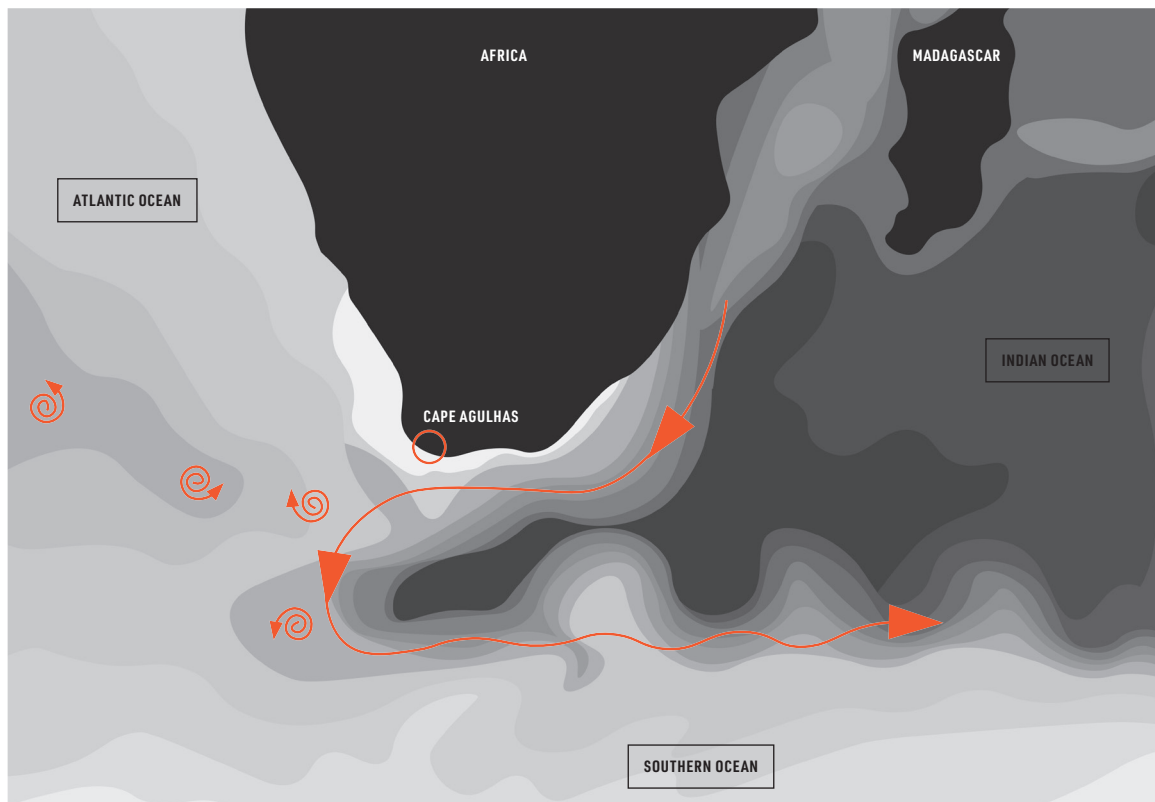
The Antarctic Circumpolar Current dominates large parts of the Southern Ocean. It is a unique flow, since it passes all longitudes (see also pages 52–53). Its strongest flow is near the surface, since it is wind-driven, but substantial magnitude still reaches into the deep sea. The relatively warm water prevents the formation of dense water. Instead, deep, dense Antarctic water

is formed in austral winter in adjacent seas, such as the Weddell Sea and the Ross Sea, which have wide openings to the deeper basins to their north. As these seas average 1,640 ft. (500 m) deep, the formed dense waters exit the seas down the continental slopes into the deeper-sea basins. The topography is thus important for the transport of different water masses and their suspended matter and nutrients.

Marginal, nearly closed-off basins

Other deep-sea basins are marginal seas that are connected to oceans via relatively small openings. Some of these marginal seas are largely deep sea. For example, the Sea of Japan reaches down to 5,740 ft. (1,750 m), the almost closed-off Black Sea to 7,220 ft. (2,200 m), and the Mediterranean Sea, at its deepest point, to about 17,225 ft. (5,250 m) below sea level. Similar to the hadal trenches (see page 74), these deepest points are not widely spread, flat seafloors but merely localized deep spots or holes, like an isolated mountain summit.

Marginal seas have characteristic deep-sea density stratification, water-flow circulation, and redistribution of matter and marine life, as in the ocean interior. However, some specific characteristics occur only in these seas.

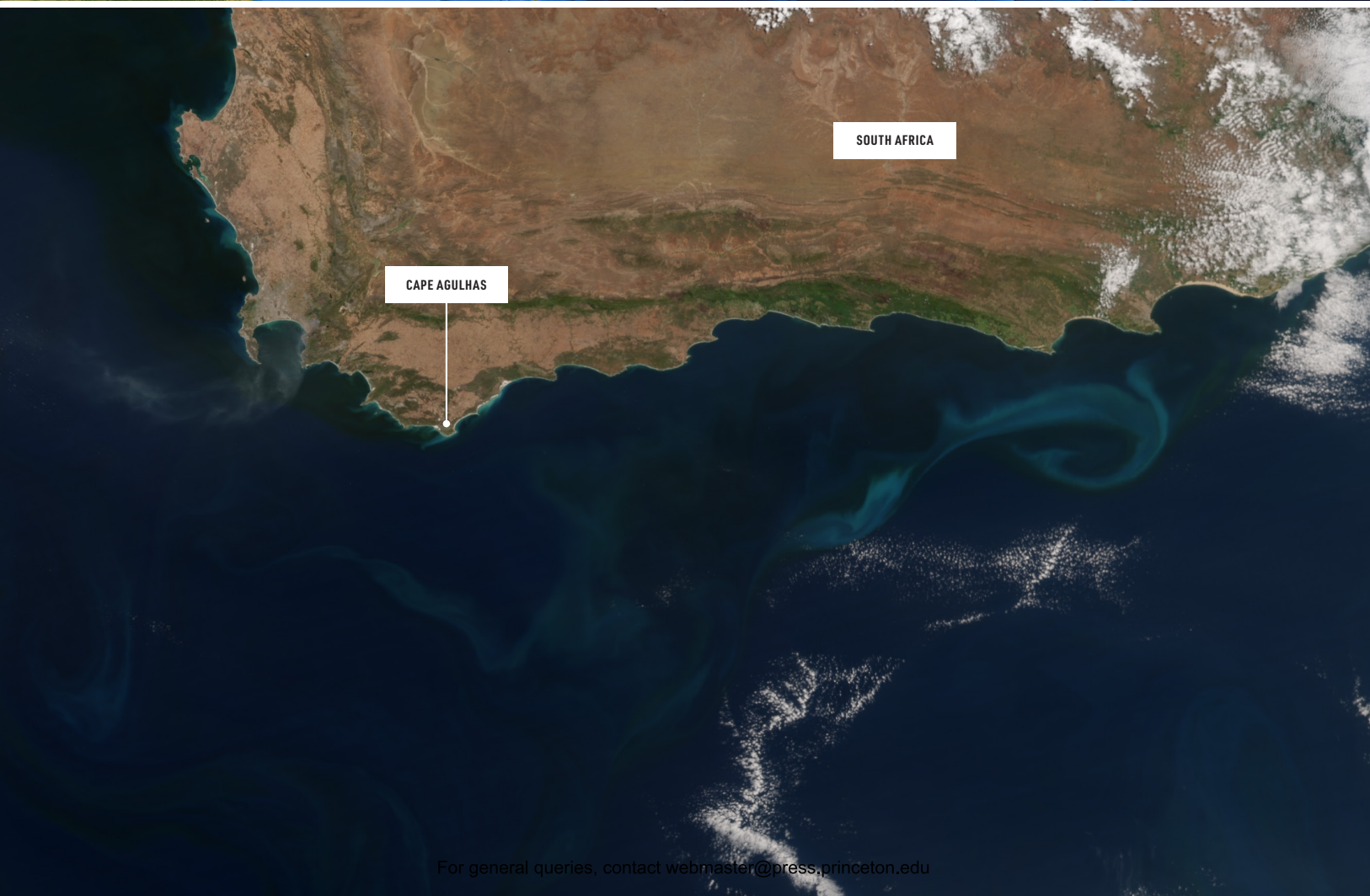


Sea of Japan

Top right: the Sea of Japan, also called the East Sea, is the marginal sea between the Japanese archipelago, Russian mainland, and the island of Sakhalin, the Korean Peninsula, and the mainland of the Russian Far East. Via sea straits between islands it is connected to the Pacific Ocean, the Sea of Okhotsk, and the East China Sea.

Agulhas Current, turning and eddies

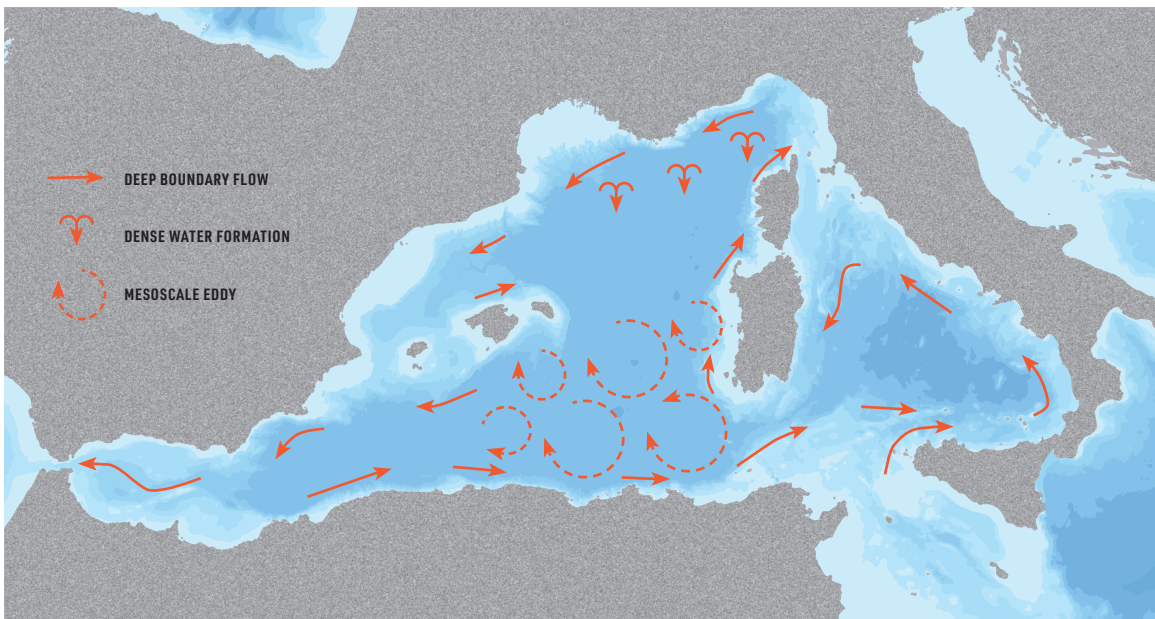
Left and bottom right: Indian Ocean flow along the east African coast collides with Atlantic Ocean waters and diverges in the direction of the Antarctic Circumpolar flow. Many eddies spin off (left). This turbulence draws nutrients for phytoplankton up from the deep; the light blue swirl to the east of Cape Agulhas in the satellite image opposite shows a phytoplankton bloom in an area of cool, upwelling water.



Tides in marginal seas

As connections to oceans are small, tides are generally weak in marginal seas. This is because in such basins, tides can be directly forced only via Earth–moon (and sun) interaction and not driven to resonance—a reinforcing of a wave at a particular frequency determined by the size of a basin—via tidal current flows at their boundaries. The boundaries or openings to adjacent larger tide-containing basins are generally too small. If we compare the Bay of Fundy, along the eastern North American coast, where the world’s largest tides are found, with the Mediterranean Sea, we notice that the Bay of Fundy has a wide opening along its entire southwestern boundary, whereas the Mediterranean has a relatively small opening in the Strait of Gibraltar. Inside the

Mediterranean near Gibraltar, tides are not negligible, but in the remainder of this marginal sea they are, with some exceptions—for example, near northern Italy, where tides are driven to resonance. Even in ocean basins, the tide-generating forces hardly directly drive tides. This is because the basin forms and scales do not fit the 6,200-mi. (10,000-km) scale of the tide. An exception is the Antarctic circumpolar basin, although even the potential direct tide-generation there is supported by some basin resonance. Nearly all ocean-surface tides of substantial amplitude are formed via resonance, in a generally complex way that is distantly reminiscent of the sound-producing resonance of organ pipes.



Flow characteristics

Left: the Mediterranean Sea shows important flows that are also characteristic for the ocean: strong boundary flows, eddies, and deep, dense water formation, which is rarely found outside the polar regions.

Bay of Fundy and Mediterranean boundaries

Examples of boundary seas to the same scale: bottom far left, the semi-enclosed Bay of Fundy with the largest tides in the world and bottom left, the Strait of Gibraltar, which exchanges Atlantic and Mediterranean waters.



(continued...)

INDEX

A

abyssal circulation 39
 abyssal ecoregions 190
 abyssal plains 23, 46, 146–53, 181, 216, 220, 221
 abyssopelagic layer 174
 acidification 15, 131, 266–71
 acidity 22, 50
 acorn barnacles 86
 acorn worms 86, 103, 152, 190
 acoustic exploration 245, 264
 adaptations 94, 110–21, 269
 Adélie Penguins 203
 Agassiz, Alexander 39
 Agulhas Current 52, 68
 airplanes 275
 albatrosses 144
 Albert I of Monaco, Prince 39
 Aldabra 260
Alicella gigantea 86, 156, 161
 allopatric speciation 226
 Alvin 40
Alvinella pompejana 162, 192
 amphipods 86, 148, 156–7, 216, 222, 263
 anemones 82
 anglerfishes 109, 118
 animal forests 127, 132, 136
 Annelida 79, 86
 anoxic events 222
 Antarctic circumpolar basin 70
 Antarctic Circumpolar Current 21, 52, 54, 61, 68, 186, 196, 207
 Antarctic glaciation 222
 Antarctic Herring 200, 203
 Antarctic icefishes 113
 Antarctic invertebrates 197
 Antarctic megafauna 203
 Antarctic shelf 196
 antifreeze glycoproteins 200
Aphanopus carbo 232
Aptenodytes 101
Aptenodytes forsteri 203
Aptenodytes patagonicus 203
 archaea 50, 158, 164
Architeuthis dux 24, 144, 245, 264
 Arctic Ocean 206–11, 256
 Arctic Ocean Diversity Project (ArcOD) 210
 Arnoux's Beaked Whale 203
 arrow worms 99, 140
 Arthropoda 79, 86, 103
 Atlantic Footballfish 104
 Atlantic Ocean
 · acidification 270
 · basin 67
 · floor 44
 · hydrothermal vents 162
 · radioactive waste disposal 256
 · radiocarbon dating 254
 Atlantification 210
 autonomous underwater vehicles (AUVs) 35
 azoic hypothesis 37

B

back-arcs 23
 Backus, Richard 40
 bacteria 50
 · mats 127, 158
 · photophores 118
 · see also chemosynthetic ecosystems; microbes
 baits 32
Balaena mysticetus 210, 241
 Ballard, Bob 40
 Baltimore Canyon 133
 bamboo corals 82, 212
 barnacles 192
 barreleyes 106

Barton, Otis 39
 Basamuk Canyon 258
 basins 55, 66–75, 206, 207
 bathyal ecoregions 190, 216, 220
Bathymodiolus 164, 182, 192
Bathynomus 86, 110
 bathypelagic layer 174
 bathysphere 39, 40
 Bay of Fundy 70
 beaked whales 35, 101, 144, 203, 241, 264
 Beaufort Dyke 256
 Beebe, William 39
 Beluga 210
 benthic boundary layer 147, 176
 benthic ecoregions 190–1
 benthic zone 16, 26
 · Arctic 210
 · fish 88–91
 · invertebrates 78–87
 · sampling 32
 · vertical zonation 212–17
Berardius amuxii 203
 Bering Strait 207
 bicarbonate 50
 biodiversity 218–21
 bioluminescence 12, 32, 50, 104, 113, 118–121, 170, 212, 228–9
 birds 144
 bivalves 86, 132, 148, 156, 164
 blackchins 228
 black corals 82
 Blackmouth Catsharks 128
 Black Scabbardfish 232
 Black Sea 68, 73, 252
 bluefin tunas 170
 blue whittings 236, 238
 Boarfish 234
 bobtails 100
 bony fishes 90–1
 bores 63
 Bosphorus Strait 73
 bottom trawling 131, 238, 270
 boundary flows 55, 71, 72
 Bowhead Whale 210, 241–2
 box jellies 97, 114
 brisingid sea stars 84
 bristlemouths 106, 228
 bristle worms 148, 154
 brittle stars 84, 103, 156, 222
 Broecker, Wallace 39
 Brunn, Anton 39
 bubble streams 30
 buoyancy 12, 88, 94, 110, 144, 150, 182, 200, 214
 buoyancy chambers 110, 214

C

calcium 50
Calyptogena 164
 cameras 32
 camouflage 94, 104, 228
 Canadian Basin 207
Cancer borealis 124
 canyons 55, 61, 71–2, 80, 124, 126–7, 131, 132–7, 181, 184, 258, 260
Capros aper 234
 carbonate compensation 214
 carbon flux 64
Carcharodon carcharias 170
 cargo ships 275
 cartilaginous fishes 88
 catsharks 88
 Census of Marine Life (CoML) 40
 Central Indian Ridge 55
Centrophorus squamosus 139
Centroscymnus coelolepis 232
 cephalopods 100, 103, 113, 114, 156, 194
 ceriantharians 82

chaetognaths 99
 Challenger Deep 35, 40, 46, 154, 264
Challenger, HMS 37
 chemoreceptors 117
 chemosynthetic ecosystems 29, 40, 86, 127, 158–67, 181, 184, 220, 241, 275
 Chernobyl incident 252
 chimaeras 88
 Chondrichthyes 88
 chromatophores 228
Chrysomallon squamiferum 162
 Chun, Carl 39
 circulation
 · abyssal 39
 · radiocarbon dating 254
 · radionuclide tracers 252
 · thermohaline 182, 222
 · World Ocean Circulation Experiment 39
Cirrothoema murrayi 113
 Cladorhizidae 80
 clams 132, 148, 156, 164
 climate change 131, 173, 209, 210, 266–71
 clinker 152, 256
 cnidarians 79, 82–3, 97
 cobalt 249, 250
 cods 90
 coelacanths 220
 cold seeps 40, 127, 158, 164, 182, 184, 192, 258, 269
Colossendeis colossea 86
 comb jellies 97
 continental drift 39, 40
 continental plates 44–6, 158
 convection 21
 Cookie-cutter Shark 104
 copepods 148, 224
 corals 79, 82–3, 127, 132–3, 136, 139, 184, 212
 · acidification 270–1
 · bottom trawling 238
 · Deepwater Horizon disaster 247
 · gardens 131, 133, 139
 · mounds 128
 · NOAA survey 194
 · plastic 263
 · reefs 128
 · speciation 224
 · summits 140
 · whale fall 167
 corers 32
 Coriolis effect 21, 52, 54, 60–1
 Corliss, Jack 40
Coryphaenoides 90, 216
Coryphaenoides rupestris 124, 140, 234
 cow sharks 88
 crabs 32, 82, 86, 124, 164, 192
 crocodile icefishes 200
 crustaceans 80, 86, 99–100, 103, 114, 127, 148, 156, 181, 190, 197, 216
 · Arctic 210
 · bioluminescence 118
 · see also amphipods; copepods; crabs; krill; lobsters; shrimps
 ctenophores 97
 currents 15, 18, 21, 23, 31, 46, 52–65, 182, 186, 224
 cusk eels 84, 90, 136, 150, 157
 cutthroat eels 90
 Cuvier's Beaked Whale 35, 144, 264
 cyanobacteria 50

D

Dasyscyopelus asper 228
 deep gliders 35
 deep scattering layer 39, 40, 106, 124, 136, 140, 170, 181
 deep-sea flows 54–5, 57
 deep-sea tailings disposal (DSTD) 258
 deep sinking 72–3
 Deep Water Dump Site 106 256

Deepwater Horizon disaster 247, 270
defense strategies 117, 118
Delphinapterus leucas 210
demosponges 79, 80
dense water-mass formation 56–7, 72
density 48, 52, 54–5, 57, 72–3
depth
· speciation 224
· zones 16
Dermochelys coriacea 101, 170
Desmophyllum dianthus 184
Desmophyllum pertusum 82, 128, 140, 263, 270
digestion 110
dispersal 182, 184, 189
Dissostichus 200
Dissostichus eleginoides 234
dogfish sharks 88
dolphins 101, 104, 144
Dosidicus gigas 189, 228
dragonfishes 106, 118, 144, 228
dredges 32, 37
drill mud 247
dwarfism 29
dynamic positioning 247

E

earthquakes 46, 154, 264
Eastern Tropical Pacific 189, 226
echinoderms 79, 84–5, 103, 114, 127, 156, 222, 269
echinothuriids 84
ecoregion classification 186–95
ecosystems
· connected 180–95
· see also chemosynthetic ecosystems
eddies 31, 54, 68, 71, 168
elpouts 90, 200, 210
eels 39, 84, 90, 104, 108, 136, 150, 157
Ekman, Vagn Walfrid 39
electrical receptors 117
Electrona antarctica 186
elephant seals 35, 101, 203
Emperor Penguins 203
endangered species 162
energy management 110
Eschrichtius robustus 241
Eubalaena 241
Euphausia superba 197
Eurypharynx pelecanoides 108
evaporation 72
evolutionary relationships 29
extinction events 220, 222
eyes 114
eyespot 114

F

faunal data 188–9
feather stars 84, 103
feeding 29
· continental slopes 124
· ecosystems 181
· trenches 157
· zonation 216–17
feeling 117
ferromanganese crusts 23, 249, 250
finned octopods 100
fishes 37, 110, 194
· abyssal plains 150
· Arctic and Antarctic 210
· benthic 88–91
· biodiversity 221
· bioluminescence 228
· canyons 136

· continental slopes 124
· ecoregions 190
· electroreceptors 117
· eyes 114
· mesopelagic 40
· pelagic 104–9
· Southern Ocean 200
· speciation 224
· summits 140, 142
· trenches 157
fishing 131, 232–9, 270
flatfishes 90
flux studies 40
foraminifera 148, 154
Forbes, Edward 37
fracture zones 55, 57, 74, 152
frilled sharks 88
fronts 186
fulmars 144
fungi 24

G

Galathea 39
Galeus melastomus 128
gas hydrates 251
Gazelle 39
ghost sharks 220
Giant Squid 24, 144, 245, 264
giant viruses 24
Gibraltar, Strait 70
gigantism 29, 82, 197
Gigantocypris 114, 156
Glacial Eelpout 210
glass sponges 79, 80
glass squid 194
gliders 35
Globicephala melas 144, 264
Goblin Shark 104
grabs 32
Gray Whales 241–2
great ocean conveyor 39, 182
Great White Sharks 170
Green Bomber Worm 118
Greenland coral gardens 133
Greenland Halibut 232, 236
Greenland Shark 88, 232
grenadiers 90, 124, 136, 140, 150, 157, 194, 200, 216, 224, 234, 238
Guam 35
Gulf of Alaska 234
Gulf of Mexico 189, 218, 224, 270
Gulf Stream 52, 54, 71
guyots 46
gyres 52, 68, 182, 186

H

habitat 26, 122–77
hadal ecoregions 190
hadal trenches 46, 74, 90, 154–7, 176, 190
hadopelagic zone 176
hagfishes 88, 166–7
halibuts 90, 124
halosaurs 90
harpacticoid copepods 148
hatchetfishes 106, 228
Hawaiian Islands 23, 124, 142, 194
hearing 117
heart urchins 84
Heezen, Bruce 40
hemocyanin 113
hemoglobin 158, 167, 200, 203
hexactinellid sponges 79, 80

Himantolophus groenlandicus 104
Hirondellea 157
histioteuthid squids 114
hoki 236
holoplankton 99
Honjo, Susumu 40
Hoplostethus atlanticus 142, 234
hot-spot volcanism 23
Hovis, Warren 40
human-occupied vehicles (HOVs) 35, 40
humans 8, 15, 230–75
Humboldt Squid 189, 228
Humpback Whale 35, 241–2
hydraulic dredging 249
hydraulic-jump mixing 64
hydrothermal vents 40, 158, 162, 184
· acidification 269
· ecoregions 192–3
· jurisdiction 251
· sulfide deposits 249, 250
hydrozoans 82, 97
Hyperoodon ampullatus 136

I

ice algae 209
icebergs 209
ice dynamics 209
incirrate octopods 100
Indian Ocean
· basin 68
· floor 44
“intermediate-disturbance” hypothesis 220
internal waves 18, 21, 23, 57, 60–4, 71, 271
· breaking 61–3
· canyons 127, 136
· kinetic energy 39
marginal seas 71
International Seabed Authority (ISA) 251
invertebrates
· Antarctic 197
· pelagic 94
Ipnops 114
iron 22
Isistius brasiliensis 104
isopods 86, 110, 148, 216
isopycnals 57, 64

J

jawless fishes 88
jellyfishes 97, 99
jet stream 21
Jonah Crab 124

K

Kaikōura Canyon 136
kinetic energy 60–1, 71, 73
King Penguins 203
kitefin sharks 88, 104
Kiwa tyleri 192
krill 100, 101, 106, 108, 136, 140, 144, 186, 197, 203
Kula oceanic ridge 192
Kuroshio Current 52, 54, 61, 71

L

Lamellibrachia 164
 landers 32
 lanternfishes 106, 144, 186, 194, 200, 228
 lantern sharks 104, 200
 Laplace, Pierre-Simon 36
 larvaceans 98
 larvae 182–4, 197
Latimeria 220
 Leafscale Gulper Shark 139
 Leatherback Sea Turtle 101, 170, 173
lebensspuren (life signs) 86
 lecithotrophic larvae 182
Leiogalatea 222
Leptomychotes weddellii 203
 lidar 31
 light
 · zonation 212
 · see also bioluminescence
 lightfishes 106
Limacina helicina 210
 limpets 192
 litter 260–3
 lizardfishes 90, 106
 lobsters 86, 110, 222
 Longfinned Pilot Whales 144, 264
 longlines 32
 lophogastrids 100
 lures 32
Lycodes frigidus 210

M

macrofauna 148
Macropinna microstoma 106, 114
Macruronus 236
 magma 46
 magnetic fields 117
Malacosteus niger 113
 manganese nodules 23, 152, 249, 251
 mantle plumes 23
 marginal seas
 · basins 68–72
 · subbasins 74
 Mariana Snailfish 35, 90
 Mariana Trench 35, 40, 46, 90, 154, 260, 264
 marine litter 260–3
 marine snow 80, 98, 127, 140, 146–7, 181
 mate choice 228
 Matthews, Drummond 40
 mechanoreceptors 117
 Mediterranean Sea 68, 70, 72, 73, 74, 189, 215
 megafauna 150
 megaplankton 99, 101, 110, 210
Megaptera novaengliae 35, 241
 meiofauna 148, 154
Merluccius 236
 meroplankton 99
 mesopelagic boundary community 124
 mesopelagic layer 170, 181, 224
 · ecoregion classification 186–9
 · fish 40
 mesoscale eddies 68, 71
 Messina, Strait 74
 methane 251
 microbes 29, 50
 · pelagic 94
 · see also bacteria; chemosynthetic ecosystems
Micromesistius 236
 micronekton 100, 186, 228
 micronutrients 22
 microplastic 263
 Mid-Atlantic Ridge 44, 46, 55, 67, 74, 139, 162, 234
 mid-ocean ridges 40, 46, 57, 67, 74, 138–9, 158
 migration 144, 216, 222
 · magnetic fields 117
 · vertical 31, 100, 140, 170, 176, 181, 209, 210, 247
 minerals 22, 23, 46, 181
 mine tailings disposal 258
 mining 244–51
Mirocaris 192

Mirounga 101
Mirounga angustirostris 35
Mirounga leonina 35, 203
Mitsukurina owstoni 104
 Mollusca 79, 86, 148, 156
 · see also cephalopods; clams; snails
 monkfishes 124
Monodon monoceros 210
 morids 194, 200
 Morley, Lawrence 40
 munitions dumps 256
 Murray, John 37
 mussels 164, 182, 192

N

Narwhal 210
 National Oceanic and Atmospheric Administration (NOAA) 194
Nautilus 214
 nekton 99–101
 nematode worms 148, 154
Nemichthys scolopaceus 104
 nepheloid layers 136
 net sampling 32
 noise pollution 264–5
 Northern Bottlenose Whales 136
 Northern Elephant Seal 35
Notoliparis 157, 200
Notoscopelus bolini 228
 notothenioids 200
 nuclear bomb testing 254
 nudibranchs 99

O

Oarfish 24
 oceanic plates 44–6
 oceanography 42–75
 octocorals 82, 133
 octopods 86, 100, 110, 117, 156, 158
Odobenus rosmarus 210
 oil see petrochemicals
 Oilfish 232, 234
 Orange Roughy 142, 234, 238
 Orcas 210
Orcinus orca 210
 oreos 194
Osedax 167, 182, 241
 ostracods 114, 148
 ostur 131
 oxygen 15
 · anoxic conditions 73
 · hydrographic mapping 39
 · metabolism 113
 · saturation 48
 · zonation 215
 oxygen-minimum zones (OMZs) 15, 39, 48, 66–7, 127, 173, 189, 215, 226
 oysters 132

P

Pacific Ocean
 · abyssal plains 152
 · acidification 270
 · basin 67
 · floor 44
 · hydraulic dredging 249
 · plate 46
 Pacific Ocean Perch 234
 Pacific Plate 44
 paleogeomagnetic studies 40
 Panamanian Seaway 192
Paraliparis 200
Paramuricea 224
 Patagonian Toothfish 234

Paull, Charles 40
 peanut worms 79, 86
 pearleyes 106
 pelagic zone 16, 26
 · biodiversity 220, 221
 · canyons 136
 · fish 104–9
 · organisms 94–109
 · sampling 32
 · trawling 238
 Pelican Eel 108
 penguins 94, 203
Pentaceros wheeleri 142, 234
 perch 236
 petrels 144
 petrochemicals 244–51, 270
 pheromones 117
 Philippine Trench 39
 photophores 118, 228
Physeter macrocephalus 24, 101, 117, 136, 144, 203, 241
 phytoplankton 12, 31, 71, 127, 140, 146–7, 181, 209
 Picasso Sponge 131
 Piccard, Jacques 40
 piezolytes 214
 pilot whales 101, 144, 264
 planktonic larval duration (PLD) 182
 planktotrophic larvae 182
 plastics 8, 15, 260–3
 plateaus 138–45
 Polar Bears 209, 210
 polar front 186
 polar seas 194, 196–211
 polychaete worms 79, 86, 114, 148, 154, 226
 Pompeii Worm 162, 192
 Porifera 79, 80–1
 Portuguese Dogfish 232
 pressure 21, 32, 52, 54, 174
 · feeling 117
 · metabolism 113
 · zonation 214
 Pressure Drop ship 35
Prestige 247, 272
 Prickly Lanternfish 228
 provinces 192
Pseudoliparis swirei 35, 90, 157
Psychropotes 150
 pteropods 99, 210, 269
 Pudgy Cusk Eel 90
 Puerto Rico Dump Site 256
 pyrosomes 98

R

radioactive contamination 252–6, 272
 radiocarbon dating 254
 radionuclides 252
 Ram's Horn Squid 100
 ray-finned fishes 90
 rays 88, 139, 200
 reefs 82
 refuges 220
Regalecus glesne 24
Reinhardtius hippoglossoides 232
 remotely operated vehicles (ROVs) 35, 40, 128, 132, 194, 250
 remote sensing 40
 reproduction 182–4
 · larvae 182–4, 197
 · mate choice 228
 resonance 70
Reticulammina 150
Ridgeia piscesae 192
 ridges 40, 44–6, 57, 67, 74, 138–45, 158
 · Mid-Atlantic Ridge 44, 46, 55, 67, 74, 139, 162, 234
 · turbulence 64
Riftia pachyptila 158, 192
 right whales 241–2
Rimicaris 114
Rimicaris exoculata 162, 192
 Risso, Antoine 37, 212
 robotic vehicles 35
 Ross, Captain James Clark 37
 Ross, John 37
 Ross Sea 68

roughies 194, 234, 238
Roundnose Grenadier 124, 140, 234, 238
rusticles 272
Ruvettus pretiosus 232

S

sabertooth fishes 106
Saccopharyngidae 108
salinity 15, 21, 22, 31, 32, 39, 48, 50, 67
salps 98
sampling 32
Sandalops melancholicus 194
Sandwell, David 40
Sars, Michael 37
satellites 31, 40, 232, 247
sawtooth eels 108
scale worms 118
Scaly-foot Snail 162
Schmidt, Johannes 39
schreckstoff (fright substance) 117
sclerites 82
Scotoplanes 84
sea cucumbers 15, 84, 103, 110, 118, 147, 150, 156, 167, 190, 216, 222, 269
sea elephants 99, 100
sea fans 82
sea ice 206, 209
Sea of Japan 68
sea lilies 84, 110, 156, 222
seals 203, 210
seamounts 23, 46, 66, 80, 138–45, 181, 190
· biodiversity 220
· ferromanganese crusts 249, 250
· jurisdiction 251
· litter 260
· stepping-stones 184
Sea Pangolins 162
sea pens 82, 131, 212
sea pigs 84
sea spiders 79, 86, 103, 197
sea stars 124, 156, 222
sea urchins 84–5, 156
Sebastes 236
Sebastes alutus 234
Secchi disk 203
seed shrimps 114, 148
selection 224, 226
semisubmersible platforms 247
sessile species 29
sharks 35, 88, 104, 110, 128, 139, 166–7, 170, 200, 220, 232
shipping containers 275
shipwrecks 272–5
shrimps 100, 114, 136, 148, 162, 164, 192, 236
Sicily, Strait 74
siphonophores 94, 97, 99, 171–2
size
· groupings 29
· zooplankton 99
skates 88, 158
Slender Armorhead 142, 234
Slender Snipe Eel 104
slickheads 90
slopes 62–3, 124–7, 128, 131
smelling 117
smelts 90, 106
Smith, Walter 40
snailfishes 35, 90, 157, 200
snails 84, 99, 110, 114, 148, 156, 162, 192, 210
snipe eels 108
sofar 48
solar energy 18, 56, 60, 212
Solenosmilia variabilis 140, 184
solibores 63
Somniosus microcephalus 88, 232
sonar 30, 39, 132, 170, 232, 245, 264
Southern Elephant Seal 35, 203
southern hakes 236
Southern Ocean 68, 192, 196–203, 207, 209, 210
sparkers 245
speciation 222–9
Spectrunculus grandis 90

speed of sound 48
Sperm Whale 24, 101, 117, 136, 144, 203, 241
spiny eels 90
Spirula spirula 100
sponges 79, 80–1, 110, 127, 131, 139, 140, 197
spookfishes 106, 114, 115
spoon worms 152
squid 24, 100, 110, 114, 118, 124, 136, 144, 156, 189, 194, 197, 203, 228, 245, 264
Stannophyllum zonarium 150
Staurocalyptus 131
“stepping-stone” hypothesis 184
Stommel, Henry 39
stony coral 82, 128
stoplight loosejaws 106, 113
stromatolites 50
subbasins 74
subduction zones 44, 46, 74, 158
submersibles 35
sulfide deposits 249, 250
sulfur-hexafluoride tracer 252
Swima bombaviridis 118
swim bladders 117, 200, 214
symbiosis 162
sympatric speciation 226
Symphurus 90

T

Talisman 39
tanaids 148
Taonius pavo 194
tardigrades 148
tectonic plates 23, 39, 40, 44–6, 74, 222
telegraph cables 39
telescopefishes 106
temperature 15, 31
· hydrographic mapping 39
· oxygen 173
· pressure effect 21
· zonation 215
· see also climate change
Tethys Sea 192, 222
Teuthowenia maculata 194
Teuthowenia megalops 194
Tharp, Marie 40
thermohaline circulation 182, 222
thiotrophic microbes 158
Thompson, Charles Wyville 37
Thunnus 170
tides 36, 60–1
· marginal seas 70
· tidal energy 271
Titanic 272
tonguefishes 90
toothed whales 101, 117, 136, 144, 173, 241
toothfishes 200, 234
topography 23, 30, 40, 44–7
· basins 66–75
· slopes 62–3, 124
· trenches 74
toxicity 162
traps 32
Travailleur 39
trenches 7, 23, 30, 46, 64, 74, 154–7
Trieste 40
tripod fishes 90
tube anemones 82
tube worms 79, 86, 158, 164, 182, 192
tunas 170
tunicates 98, 99
turbulent mixing 21, 23, 39, 46, 48, 52–65, 66, 74, 252, 271
typhoon (hurricane) 62, 264

U

United Nations Convention on the Law of the Sea (UNCLOS) 251
Ursus maritimus 209, 210

Vampire Squid 118
Vampyroteuthis infernalis 118
vent shrimps 162, 192
Vine, Frederick 40
vipercodfishes 106
viruses 24, 50
vision 113–14
Vityaz 39
volcanic arcs 23, 46
volcanic ridges 46
volcanic vents 50
volcanism 23
Vulnerable Marine Ecosystems 127, 128, 131–2, 238

W

Walrus 210
Walsh, Don 40
waste disposal 256–63
water column 168–77
water-mass formation 56–7
water sampling 32
Weddell Sea 68
Weddell Seals 203
Wegener, Alfred 39
whale fall 166–7, 181, 184, 241, 242
whalefishes 109
whales 101, 117, 136, 144, 173, 203, 210, 264
whaling 240–3
whip corals 212
Whittard Canyon 61, 132, 133–4
wind 52, 54, 60–1, 72, 186
Woods Hole Oceanographic Institution (WHOI) 40
World Ocean Circulation Experiment (WOCE) 39

X

xenophophores 86, 150

Y

yeti crabs 192

Z

Ziphius cavirostris 35, 144, 264
zoantharians 82
zombie worm 167
zonation 212–17
zooplankton 32, 90, 99, 127, 140, 147, 181, 186, 210